12-2020

Influences of Forest Edges on the Growth and Health of Old-Growth Coast Redwood Forests

Cody R. Dangerfield
Utah State University

INFLUENCES OF FOREST EDGES ON THE GROWTH AND HEALTH OF OLD-GROWTH COAST REDWOOD FORESTS

by

Cody R. Dangerfield

A thesis submitted in partial fulfillment
of the requirements for the degree

of

MASTER OF SCIENCE

in

Ecology

Approved:

_____	_____
Steve Voelker, Ph.D. Co-Major Professor	Larissa Yocom, Ph.D. Co-Major Professor
_____	_____
James A. Lutz, Ph.D. Committee Member	Pat Terletzky, Ph.D. Committee Member

_____

D. Richard Cutler, Ph.D.
Interim Vice Provost of Graduate Studies

UTAH STATE UNIVERSITY
Logan, Utah

2020

ABSTRACT

Influences of Forest Edges on the Growth and Health of Old-growth Coast Redwood Forests

by

Cody R. Dangerfield, Master of Science

Utah State University, 2020

Co-Major Professors: Dr. Steve Voelker and Dr. Larissa Yocom
Department: Wildland Resources

The coast redwood (*Sequoia sempervirens*) ecosystem has been heavily fragmented following extensive logging and landcover changes in the 19th and 20th centuries. These activities have created abrupt forests edges throughout the redwood's range, leaving the remaining stands exposed to elevated temperature, sunlight, and wind intensities, thereby making redwoods along the forest edge more susceptible to windthrow and drought stress. Despite the rarity of old-growth coast redwood forests and their ecological and cultural significance, very few studies have investigated how forests edges impact the productivity and health of these forests. In these studies, we combine dendrochronology with remote sensing methods to better understand the spatial and temporal patterns of redwood stress and how it has been impacted by habitat fragmentation.

In the first study, we employed disturbance detection methods on tree-ring widths and stable carbon isotopes to determine how a previous expansion of Highway 101

through Humboldt Redwood State Park has impacted the growth and drought stress of redwoods bordering the highway. We found that the expansion of the highway disproportionately impacted the growth of trees that were within 30 m of the highway and growth declines were more severe in trees that had dieback. Our analyses of stable carbon isotopes showed that highway-adjacent trees also experienced elevated drought stress for several decades following the construction of the highway.

In the second study, we used aerial imagery and discrete return Light Detection and Ranging data (LiDAR) to map the prevalence of crown health deterioration at the individual tree level and investigate its potential drivers in Humboldt Redwood State Park. Our results indicated that the methodology was successful in detecting crown deterioration and may provide a potential avenue for conducting cost-effective health assessments in the future. Additionally, our results show that crown dieback was particularly abundant in taller trees and aggregated in areas where tree density was low and multiple anthropogenic edges bisected old-growth redwood stands.

(117 pages)

PUBLIC ABSTRACT

Influences of Forest Edges on the Growth and Health of

Old-growth Coast Redwood Forests

Cody R. Dangerfield

Coast redwood (*Sequoia sempervirens*) is the tallest species in the world, frequently attaining heights greater than 300 ft. The unique characteristics of the redwoods has led to the establishment of several preservation areas including national and state parks. However, abrupt forests edges created by previous logging and landcover changes has left the remaining stands exposed to elevated temperature, sunlight, and wind intensities, thereby making redwoods along the forest edge more susceptible to windthrow and drought stress. Despite the rarity of old-growth coast redwood forests and their ecological and cultural significance, very few studies have investigated how forests edges have impacted the productivity and health of these forests. In these studies, we combine dendrochronology with remote sensing methods to better understand the spatial and temporal patterns of redwood stress and how it has been impacted by habitat fragmentation. In the first study, we investigated how a previous road expansion has impacted the growth and drought stress of nearby redwoods. In the second study, we mapped declines in redwood crown health to better understand the relationship between crown health and environmental variables such as distance to forest edge, local tree density, and overall tree height. Our results indicated that previous road expansions caused growth declines in adjacent trees and caused elevated drought stress in the subsequent decades. Our results also indicated that taller trees were more susceptible to

declines in crown health and crown dieback was found in higher concentrations where multiple roads and previously logged areas intersect old-growth stands.

ACKNOWLEDGMENTS

The work conducted in this thesis would not have been possible without the collaboration from a number of people and I could not be more thankful for their input and assistance. First, I would like to thank my co-advisers Steve Voelker and Larissa Yocom, for their support and advice throughout my entire thesis, and admittedly, letting me show them too many figures. I would also like to thank my committee members Pat Terletzky and Jim Lutz for their helpful guidance.

I would also like to thank the plethora of faculty, staff and graduate students that spoke with me about my project during my time at USU: Tucker Furniss, Susan Durham, Gustavo Ovando-Montejo, Juergen Symanzik, Curtis Gray, Will Pearse, Doug Ramsey, Kezia Manlove, Karen Mock, and Justin DeRose. I gained several insights from each of our correspondences and this thesis has greatly benefited from their guidance. I would also like to thank my lab mates Rachel Keen, Maria Catalano, Mark Kreider, Alex Howe, and Jamela Thompson for their help workshopping ideas, advice on classes, and their overall perspectives.

Thank you to our funding sources Save the Redwoods League, the USU Ecology Center, and the USU Office for Graduate Research. Without their support, this research would not have been possible.

To my family, I would not be where I am without your support and encouragement. Lastly, I would like to thank McKaela Forbush for being there for me through all the edits, practice talks, ramblings, and being willing to take spontaneous panic trips to the redwoods to collect data.

Cody R. Dangerfield

CONTENTS

LIST OF TABLES

Page

LIST OF FIGURES

Page

CHAPTER 1

INTRODUCTION

Coast redwood (*Sequoia sempervirens*) is a strictly mesophilic species whose distribution has historically relied on a mild mesic climate with minimal exposure to drought (Sawyer et al., 2000). Following cooling and drying changes in climate during the Cenozoic era (Pittermann et al., 2012), the redwood distribution contracted to the coastal region of California and a small portion of Oregon where it appears reliant on hydrologic input from coastal upwelling and fog inundation to persist on the landscape (Johnstone & Dawson, 2010; McLaughlin et al., 2017). The coastal range has provided a stable climate for the species and has served as a hydrologic refugium during the most severe droughts of the past millennia (Voelker et al., 2018). In recent decades, decreases in precipitation have caused widespread elevated rates of tree mortality across multiple species, and these trends are projected to continue (Allen et al., 2010). Although conditions of a near-coastal climate have buffered redwoods from previous droughts, fog frequency has been in decline for nearly a century and it remains unclear how temperature increases will impact fog moving forward. Accordingly, the future of redwoods is unknown (Cordero et al., 2011; Fernández et al., 2015; Johnstone & Dawson, 2010).

Habitat fragmentation caused by previous timber harvests and land cover changes to roads, agricultural fields, and residential areas also pose threats to the health and composition of the redwood ecosystem (Burns et al., 2018; Russell et al., 2000). These landcover conversions have created isolated stands with abrupt forest edges that experience elevated intensities of sunlight, temperature, and wind, and in the case of

roads, potential root damage and soil compaction. The increased exposure associated with these edges has been found to cause elevated rates of crown dieback and windthrow, especially in taller trees (Harper et al., 2005; Laurance et al., 2009; Laurance & Curran, 2008; Laurance & Yensen, 1991; Russell et al., 2000). While the establishment of national and state parks has helped preserve the remaining extent of the redwood distribution, the conditions near forest edges have the potential to compound with climate change to negatively impact the function and structure of the remaining old-growth redwood forests (Burns et al., 2018; Fernández et al., 2015; Johnstone & Dawson, 2010; Russell et al., 2000).

While redwoods have several traits that have made them resistant and resilient to natural disturbances such fire, flood, and pests (Lorimer et al., 2009; Stone & Vasey, 1968), they also have an aggregation of traits that considerably reduce their resistance to drought. Redwoods are the tallest species in the world, but they also have a relatively shallow root system and lack of roots hairs, which limits their access and uptake efficiency of deep groundwater sources (Burgess & Dawson, 2004; Fritz, 1929; Olson et al., 1990; Stone & Vasey, 1968). Additionally, as redwoods increase in height so do the hydraulic constraints of their water column. The low water potentials in the crowns of individual redwoods increase their susceptibility to xylem cavitation which can lead to partial crown dieback or mortality (Domec et al., 2010; Koch et al., 2004). While stomatal closure can decrease cavitation risk during periods of elevated drought stress, the coast redwood is a relatively anisohydric species and lacks stomatal control (Ambrose et al., 2015; Dawson et al., 2007). It has been shown to transpire at night when there is no photosynthetic benefit (Dawson et al., 2007). This lack of water use efficiency may be

partially explained by asymmetric guard cells and endophytes that prevent full stomatal closure (Burgess & Dawson, 2004). Collectively, these physiological traits of redwoods not only emphasize the importance of a mesic climate with abundant rainfall and fog for the redwoods range, but they also suggest a potential heightened susceptibility to declines in water availability either from changes in fog frequency, reduced precipitation associated climate change, or disturbance events that increase crown exposure and/or constrict access to soil water.

While the ecological effects of habitat fragmentation have been well documented in other forest types (Goosem, 2007; Harper et al., 2005; Laurance et al., 2009; Trombulak & Frissell, 2000), more research is needed in order to elucidate the impact that forest edges have had on edge-adjacent redwoods. Towards this end, the goal of this thesis was to combine dendroecology with remote sensing to provide insights on how anthropogenic edges have influenced remaining old-growth redwood stands. Chapter 2 of this thesis uses tree-ring data (ring widths and stable carbon isotopes) to investigate the temporal and spatial impacts that a previous highway expansion through Humboldt Redwood State Park (HRSP) has had on the growth and drought stress of nearby redwoods. In Chapter 3, crown health classifications were conducted on aerial imagery and were combined with discrete return aerial Light Detection and Ranging (LiDAR) data to map individual tree crown health throughout the lowland old-growth stands of HRSP. We then analyzed the spatial patterns of crown deterioration and investigated potential drivers using environmental variables such as proximity to forest edges, local topography, local tree density, and tree height.

References

Allen, C. D., Macalady, A. K., Chenchouni, H., Bachelet, D., McDowell, N., Vennetier, M., Kitzberger, T., Rigling, A., Breshears, D. D., Hogg, E. H. (Ted., Gonzalez, P., Fensham, R., Zhang, Z., Castro, J., Demidova, N., Lim, J. H., Allard, G., Running, S. W., Semerci, A., & Cobb, N. (2010). A global overview of drought and heat-induced tree mortality reveals emerging climate change risks for forests. *Forest Ecology and Management*, *259*(4), 660–684. https://doi.org/10.1016/j.foreco.2009.09.001

Ambrose, A. R., Baxter, W. L., Wong, C. S., Næsborg, R. R., Williams, C. B., & Dawson, T. E. (2015). Contrasting drought-response strategies in California redwoods. *Tree Physiology*, *35*(5), 453–469. https://doi.org/10.1093/treephys/tpv016

Burgess, S., & Dawson, T. E. (2004). The contribution of fog to the water relations of Sequoia sempervirens (D. Don): Foliar uptake and prevention of dehydration. *Plant, Cell and Environment*, *27*, 1023–1034. https://doi.org/10.1111/j.1365-3040.2004.01207.x

Burns, E. E., Campbell, R., & Cowan, P. D. (2018). *State of Redwoods Conservation Report: A Tale of Two Forests*. https://www.savetheredwoods.org/wp-content/uploads/State-of-Redwoods-Conservation-Report-Final-web.pdf

Cordero, E. C., Kessomkiat, W., Abatzoglou, J., & Mauget, S. A. (2011). The identification of distinct patterns in California temperature trends. *Climatic Change*, *108*(1), 357–382. https://doi.org/10.1007/s10584-011-0023-y

Dawson, T. E., Burgess, S. S. O., Tu, K. P., Oliveira, R. S., Santiago, L. S., Fisher, J. B.,

Simonin, K. A., & Ambrose, A. R. (2007). Nighttime transpiration in woody plants from contrasting ecosystems. *Tree Physiology*, *27*(4), 561–575. https://doi.org/10.1093/treephys/27.4.561

Domec, J. C., Schäfer, K., Oren, R., Kim, H. S., & McCarthy, H. R. (2010). Variable conductivity and embolism in roots and branches of four contrasting tree species and their impacts on whole-plant hydraulic performance under future atmospheric CO2 concentration. *Tree Physiology*, *30*(8), 1001–1015. https://doi.org/10.1093/treephys/tpq054

Fernández, M., Hamilton, H. H., & Kueppers, L. M. (2015). Back to the future: using historical climate variation to project near-term shifts in habitat suitable for coast redwood. *Global Change Biology*, *21*(11), 4141–4152. https://doi.org/10.1111/gcb.13027

Fritz, E. (1929). Some popular fallacies concerning California redwood. *Madroño 1*, 221–224.

Goosem, M. (2007). Fragmentation impacts caused by roads through rainforests. *Current Science*, *93*(11), 1587–1595.

Harper, K. A., Macdonald, S. E., Burton, P. J., Chen, J., Brosofske, K. D., Saunders, S. C., Euskirchen, E. S., Roberts, D., Jaiteh, M. S., & Esseen, P.-A. (2005). Edge Influence on Forest Structure and Composition in Fragmented Landscapes. *Conservation Biology*, *19*(3), 768–782. https://doi.org/10.1111/j.1523-1739.2005.00045.x

Johnstone, J. A., & Dawson, T. E. (2010). Climatic context and ecological implications of summer fog decline in the coast redwood region. *Proceedings of the National*

Academy of Sciences of the United States of America, *107*(10), 4533–4538. https://doi.org/10.1073/pnas.0915062107

Koch, G. W., Stillet, S. C., Jennings, G. M., & Davis, S. D. (2004). The limits to tree height. *Nature*, *428*(6985), 851–854. https://doi.org/10.1038/nature02417

Laurance, W. F., & Curran, T. J. (2008). Impacts of wind disturbance on fragmented tropical forests: A review and synthesis. *Austral Ecology*, *33*, 399–408. https://doi.org/10.1111/j.1442-9993.2008.01895.x

Laurance, W. F., Goosem, M., & Laurance, S. G. W. (2009). Impacts of roads and linear clearings on tropical forests. *Trends in Ecology and Evolution*, *24*(12), 659–669. https://doi.org/10.1016/j.tree.2009.06.009

Laurance, W. F., & Yensen, E. (1991). Predicting the impacts of edge effects in fragmented habitats. *Biological Conservation*, *55*, 77–92. https://doi.org/https://doi.org/10.1016/0006-3207(91)90006-U

Lorimer, C. G., Porter, D. J., Madej, M. A., Stuart, J. D., Veirs, S. D., Norman, S. P., O'Hara, K. L., & Libby, W. J. (2009). Presettlement and modern disturbance regimes in coast redwood forests: Implications for the conservation of old-growth stands. *Forest Ecology and Management*, *258*(7), 1038–1054. https://doi.org/10.1016/j.foreco.2009.07.008

McLaughlin, B. C., Ackerly, D. D., Klos, P. Z., Natali, J., Dawson, T. E., & Thompson, S. E. (2017). Hydrologic refugia, plants, and climate change. *Global Change Biology*, *23*(8), 2941–2961. https://doi.org/10.1111/gcb.13629

Olson, D. F., Douglass, R. F., & Walters, G. A. (1990). Sequoia sempervirens. *In Silvics of North America, Volume 1, Conifers. USDA Forest Service Handbook*, 654.

Pittermann, J., Stuart, S. A., Dawson, T. E., & Moreau, A. (2012). Cenozoic climate change shaped the evolutionary ecophysiology of the Cupressaceae conifers. *Proceedings of the National Academy of Sciences*, *109*(24), 9647–9652. https://doi.org/10.1073/pnas.1114378109

Russell, W. H., McBride, J. R., & Carnell, K. (2000). Edge effects and the effective size of old-growth coast redwood preserves. *Proceedings Rocky Mountain Research Station, USDA Forest Service*, *3*, 128–136. https://www.fs.usda.gov/treesearch/pubs/21978

Sawyer, J. O., Gray, J., West, G. J., Thornburgh, D. ., Noss, R., & Engbeck, J. . J. (2000). History of redwood and redwood forests. In *The Redwood Forest: History, Ecology, and Conservation of the Coast Redwoods.* (pp. 7–38). Island Press.

Stone, E. C., & Vasey, R. B. (1968). Preservation Of Coast Redwood on Alluvial Flats. *Science*, *159*(3811), 157–161.

Trombulak, S. C., & Frissell, C. A. (2000). Review of ecological effects of roads on terrestrial and aquatic communities. *Conservation Biology*, *14*(1), 18–30. https://doi.org/10.1046/j.1523-1739.2000.99084.x

Voelker, S. L., Roden, J. S., & Dawson, T. E. (2018). Millennial-scale tree-ring isotope chronologies from coast redwoods provide insights on controls over California hydroclimate variability. *Oecologia*, *187*(4), 897–909. https://doi.org/10.1007/s00442-018-4193-4

CHAPTER 2

IMPACTS OF ROAD DISTURBANCE ON THE PHYSIOLOGY OF OLD-GROWTH COAST REDWOOD FOREST

Abstract

In forest ecosystems, road expansions and other landcover changes create abrupt artificial boundaries that alter the microclimate along the forest edge potentially impacting growth and physiology of bordering trees. To understand how previous landcover changes and road installations has affected coast redwoods (*Sequoia sempervirens*), we used dendroecological methods to contrast tree-ring growth patterns and stable isotopes (Δ13C) of redwoods before and after a known disturbance event, the expansion of Highway 101 in the 1950s, that bisected several old-growth stands of Humboldt Redwood State Park. Increment cores were extracted from redwoods in old-growth stands that bordered the highway and other forest edges (secondary forests and agricultural fields) as well as two control areas. Disturbance detection methods and dendroclimatic modeling were then employed to identify if the expansion led to growth suppression and elevated drought stress. Evidence from our tree-ring growth data indicated that the construction of the Highway 101 disproportionality impacted the growth of trees that were within 30 m of the highway and that these effects were particularly elevated in trees with crown dieback. Similarly, climatic modeling of $\Delta^{13}C$ data from the tree-rings indicated that highway adjacent trees also experienced elevated drought stress following the construction of the highway for several decades.

Introduction

Coast redwoods (*Sequoia sempervirens*) are the tallest organisms in the world, attaining ages exceeding 2,000 years and sequestering record amounts of aboveground carbon (Van Pelt et al., 2016). These unique characteristics, coupled with the species' rarity, have led to intensive redwood conservation efforts and the establishment of several preservation areas including state and national parks (Noss, 2000). Coast redwood's current distribution is the remnant of a much larger, widespread distribution that was associated with a more mesic climate in western North America (Noss, 2000). However, following climatic shifts ~10,000 years ago and extensive logging during the 19th and 20th centuries, redwoods are now restricted to a narrow band along the coast of California and a small portion of Oregon with only 5% of its old-growth forests remaining (Burns et al., 2018).

In near-coastal zones, redwoods have been shown to rely on fog inundation and associated canopy interception and fog drip for >40% or more of their water uptake during the nearly rainless summers (Burgess & Dawson, 2004; Dawson, 1998). These cool, near-coastal conditions, associated with coastal upwelling and cold sea surface temperatures, have created a hydrologic refugium in north coastal California that has buffered these trees through severe droughts during the last 1000 years (Voelker et al., 2018). Although conservation efforts and a relatively stable near-coastal climate have helped preserve the remaining extent of coast redwoods, the future of their distribution remains unknown, particularly in locations that lie farther inland where fog-water inputs may not be as reliable. In areas adjacent to the Pacific Ocean (i.e., < 5 km distance and <500 m elevation) redwoods can occupy all topographic and geomorphic positions,

however farther inland redwoods are constrained to valley floors and adjacent toe slopes of the coast range mountains. Growth of these inland redwood sites is closely tied to spring and summer Palmer Drought Severity Index (PDSI) (Carroll et al., 2018a) and these trees presumably have greater reliance on shallow groundwater flow from adjacent slopes compared to sites where fog is more prevalent. Therefore, human disturbances, such as road expansion projects that could injure redwood roots or locally alter hydrology, threaten to compound with long-term declines in fog frequency (Johnstone & Dawson, 2010) and increase the ecohydrological stresses imposed on this species.

Although human activity recently has been the predominant source of disturbance across the redwood distribution and has severely impacted their extent since the 1850s, historically, redwoods have withstood many different types of natural disturbances such as fire and flood. Redwoods have several traits that give them both resistance and resilience to these disturbances, which has given them a competitive advantage within their range (Lorimer et al., 2009; Stone & Vasey, 1968). Mature redwoods have thick bark that allows them to survive moderately intense fires, and their ability to regenerate vegetatively via basal burls and epicormic buds allows for partial recovery from surface fires and some canopy fires (Fritz, 1932; Lorimer et al., 2009; Stone & Vasey, 1968). Redwoods can also respond to flooding by extending their existing roots and forming new adventitious roots into new mineral deposits, although extended soil saturation can lead to increased rates of mortality and crown dieback (Stone & Vasey, 1968). Additionally, redwoods have extremely rot-resistant heartwood that limits long-term damage from wood decay fungi. These traits have contributed to the species' extreme longevity (up to 2,000 years) and historical dominance within the near coastal zones

across much of Northern California, however the relatively recent modern disturbances add new complexities to the disturbance regimes of redwoods.

Following Euro-American settlement, land cover changes caused by logging and urban development left the remaining redwood distribution heavily fragmented and exposed to different types of edge effects (Burns et al., 2018; Russell et al., 2000). These abrupt transitions from intact redwood forest to residential areas, agricultural fields, and roads increase trees' exposure to sunlight, temperature, and wind which can lead to windthrow as well as increased atmospheric moisture deficits that may be associated with crown dieback (Harper et al., 2005; Laurance & Curran, 2008; Russell et al., 2000). The prevalence of roads throughout the redwood distribution has had particularly notable effects. Abandoned logging roads have led to increased rates of erosion and have acted as inciting factors for landslides (Madej, 2010). Paved roads have been associated with crown dieback because they can have amplified edge effects on redwoods through direct root damage and restrictions to lateral groundwater movement due to soil compaction (Burns et al., 2018).

Current California Department of Transportation (Caltrans) rules for potential construction impacts on trees include consideration of the “Structural Root Zone” or “Root Health Zone”. These zones are defined by a circle with a radius of 3 to 5 times the diameter at breast height (DBH) of a given tree. The International Society of Arboriculturists (ISA) has adopted a separate rule for protecting important landscape trees, often occupying urban settings, that defines the “Critical Root Zone” as 12 times the DBH of a given tree. However, it remains unclear whether the Caltrans and ISA rules are adequate for protecting coast redwoods or other species from negative impacts of

construction. While it is possible that these rules may be appropriate for some species from drier regions of California where trees maintain large taproots and must rely on deep soil water, coastal redwoods may have a heightened susceptibility to root damage due to the morphology of their roots and their extreme height. Despite being the tallest organism in the world and regularly attaining heights exceeding 80 m, redwoods have a shallow root system that can extend horizontally for > 30 m in any direction (California State Parks, n.d.) and do not maintain a tap root (Burgess & Dawson, 2004; Fritz, 1929; Stone & Vasey, 1968). In addition, redwoods are inefficient at soil water uptake due to lack of root hairs (Olson et al., 1990) and are poor regulators of transpiration (Dawson, 1998). Consequently, damage to their shallow roots may disproportionately limit water uptake in contrast to other deeper-rooted species such as the closely-related giant sequoia (*Sequoiadendron giganteum*). A disturbance event that abruptly constricts access to soil water, such as road construction, may exacerbate the difficulties that gravity and friction inflict on plant xylem anatomy, leaf morphology and leaf gas exchange in extremely tall trees (Domec et al., 2010; Koch et al., 2004). As a result, trees may be susceptible to increased rates of embolism, branch or tree-top dieback, and mortality following events that jeopardize water availability or whole tree conductance.

In 1956, the California State Highway Commission approved construction of a new section of Highway 101 that bisected Humboldt Redwood State Park (HRSP). The goal of the highway expansion was to reduce traffic in the core areas of the park while maintaining proximity to the park to sustain tourism. The older sections of Highway 101, which are much narrower and were established decades before, were designated as the "Avenue of the Giants" to serve as a scenic route through many of the old-growth groves

adjacent to the Eel River. Construction of the highway expansion began that same year and was completed in 1960. Initially it was estimated that approximately 2,000 trees needed to be removed for the building of the new highway. In an effort to avoid the removal of any redwood “giants", the highway was mostly constructed upslope of alluvial flats or diverted to the other side of the river through the construction of bridges such as the Eagle Point Viaduct (Robinson, 1964). This type of aversion construction increased costs significantly and was successful in preserving large groves of redwoods, but decades later the prevalence of crown dieback in large redwood trees conspicuously near the highway have suggested that the expansion has had a larger impact on forest health beyond immediate tree removal.

The current spatial distribution of tree mortality and crown deterioration in HRSP (see Chapter 2 for details) along roads including Highway 101 suggest that the construction of the highway in the 1950s may have resulted in severe health effects or mortality for trees bordering the road. However, since there are no long-term forest monitoring efforts in the area, other retrospective methods for cataloging past disturbances must be employed to test whether highway construction has been detrimental to forest health. Toward this end, tree-ring data provides a valuable record of trees’ physiological responses to environmental variables (Fritts, 1976). Much of the variation in tree-ring width and carbon isotopic composition can be described as an aggregate function of tree age, climate, and disturbances. By controlling or isolating the effects of climate, age, and atmospheric carbon isotope composition on tree-ring data, it is possible to reconstruct forest disturbance history (Cook, 1987).

Since the 1980s several disturbance detection methods have been developed to isolate disturbance signals in tree rings (Rubino & Mccarthy, 2004; Trotsiuk et al., 2018). Some of these disturbance detection methods have relied on abrupt increases in radial growth, known as "releases" to reconstruct disturbance events. These growth release detection methods are based on uninjured trees producing larger rings in response to an abrupt reduction in competition and/or a release of resources following a disturbance event (Lorimer & Frelich, 1989; Nowacki & Abrams, 1997). Analyzing the pattern of abrupt decreases in growth, termed "suppressions", can also be a viable method of reconstructing disturbances that have hindered growth in the surviving trees as well (Carroll et al., 2018b; Stoffel & Bollschweiler, 2008; Trotsiuk et al., 2018). In addition to ring-width patterns, tree-ring stable isotopes can provide further insight into trees' physiological responses to environmental changes such as climate, disturbance, and pollution (Gessler et al., 2018; McCarroll & Loader, 2004; Voelker et al., 2019). During carbon fixation, discrimination ($\Delta^{13}C$) against the heavier ^{13}C compared to the lighter ^{12}C is largely dependent on the ratio of photosynthesis and stomatal conductance, and therefore, stomatal constraints on leaf gas exchange induced by drought stress can be inferred at annual resolution by measuring the $\Delta^{13}C$ values in tree rings (Farquhar et al., 1989; McCarroll & Loader, 2004). Despite challenges crossdating redwoods due to complacency, missing and wedging rings, spiral wood compression, and false rings (see Carroll et al., 2014), several studies have shown that tree rings and stable isotopes of redwoods can be a valuable method for documenting fire events (Brown & Swetnam, 1994; Carroll et al., 2018b) and redwood responses to climatic variation (Burgess &

Dawson, 2004; Carroll et al., 2014, 2018a; Johnstone et al., 2013; Johnstone & Dawson, 2010; Roden et al., 2009, 2011; Voelker et al., 2018).

In this study, we employed disturbance detection methods using tree-ring data to determine whether the disturbance associated with the construction of Highway 101 led to changes in growth and ecophysiology over time in HRSP. Given the spatial clustering of crown deterioration near Highway 101 (see Chapter 3), we expected that the installation of the highway diminished access to groundwater as a result of root severance or soil compaction, and/or increased irradiance and wind-exposure for highway adjacent trees. To differentiate between these potential effects of highway construction that occurred > 50 years ago, we examined annual tree-ring growth and $\Delta^{13}C$ values of four groups of redwoods from old-growth stands including: 1) trees adjacent to Highway 101 with substantial crown dieback, 2) trees adjacent to Highway 101 with healthy crowns, 3) trees adjacent to other edge features including agricultural fields or secondary forests to act as controls for disturbance type, and 4) trees in interior forest sites to act as controls lacking both edge conditions and proximity to anthropogenic disturbances during the construction period of the new section of highway. We expected that if redwoods were impacted by increased drought stress after the expansion of Highway 101, growth suppressions and decreases in $\Delta^{13}C$ relative to the control groups would be evident after the construction period. Alternatively, if redwood trees were not impacted by reduce water availability associated with the construction of Highway 101, highway adjacent trees would not differ from control trees in growth or $\Delta^{13}C$ values.

Methods

Study Site

All research collections and measurements took place within Humboldt Redwood State Park (HRSP), CA (40.31°N, 123.98°W). HRSP is located in northwestern California and has a Mediterranean climate with wet winters and dry summers with additional hydrological input from fog advection that follows the lower Eel River valley across a distance of 30-60 km from the Pacific Ocean and inundates areas approximately 40 to 80 m above the valley floor. The area receives an average annual rainfall of 1300 mm, and has summer temperatures that range from 10-24°C and winter temperatures that range from 4-12°C. The park consists of 53,000 ha and contains approximately 17,000 ha of old-growth redwood forest, including the Rockefeller Forest, the largest contiguous tract of old-growth forest remaining. Although HRSP is much farther inland and is drier than the more northern Redwood National and State Parks, it retains the largest aggregation of tall redwoods, as approximately 80% of all known trees >107 m tall are located in HRSP (Van Pelt et al., 2016). HRSP's retention of extremely tall trees can likely be attributed to the King Mountain Range which buffers HRSP from coastal wind storms that have previously caused crown damage and windthrow events in the more northern parks that are closer to the coast (Sillett et al., 2015; Sillett & Van Pelt, 2000). HRSP is relatively narrow and runs along the Bull Creek and lower South Fork Eel River. Like most other parks, areas surrounding and within HRSP were heavily logged which has created abrupt, artificial edges along a large proportion of the remaining old-growth forest. Presently, residential and commercial properties and agricultural fields frequently

border the park in addition to Highway 101 and other tourist byways (e.g., Avenue of the Giants).

Tree Selection and Tree Size and Crown Health Measurements

In 2018, we established 19 plots in HRSP in areas of old-growth redwood forest. Plots were established at a variety of distances to the highway (11-160 m) and other edge features. Of the 19 plots, 11 plots were in areas that bordered Highway 101. The general locations of these plots were selected in areas where a portion of the trees within the stand displayed signs of health decline and crown dieback suggesting a potential link between their health and the highway's construction (Highway-adjacent trees; Figure 2-1). Four other plots were in areas bordering other edge-types including two plots near agricultural fields and two plots near secondary forest re-growing after clear-cut harvesting. Lastly, four control plots were installed >300 m from the highway. Two of these control plots were in the Bull Creek area within the Rockefeller Forest and the remaining two were near Pepperwood, CA. At each plot, we selected at least ten trees for measurement and extraction of increment cores. Each plot's central tree was selected using a random distance and azimuth from the forest edge and the next nine trees were the closest to that central tree (Figure A-1). Tree selection was limited to those that had dominant/co-dominant canopy positions (Smith, 1986) as understory trees occupy a small fraction of the total biomass in old-growth redwood forests and were expected to have exhibited different growth and tree-ring stable isotopes patterns due to limited solar irradiance. Additional trees were added to each plot when decay prevented extracting cores that contained ≥150 years of annual growth or if crown conditions could not be determined due to limited visibility in particularly dense stands.

We measured the average crown radius and diameter at breast height (DBH) with a steel tape. Tree height and estimates of crown condition were recorded for each tree based largely upon USDA Forest Service Forest Health Monitoring methods (Lee & Muzika, 2014; Voelker et al., 2008; Zarnoch et al., 2004). Tree height, the top of the live crown, and the base of the live crown, were measured for each tree using a laser rangefinder/hypsometer. Crown dieback of each tree was visually estimated as the percentage of the crown that exhibited dieback and was recorded in five percent increments (e.g. 0%, 5%, 10%). Trees from highway adjacent plots were categorized based on the presence or absence of crown dieback. Trees whose crown contained ≥5% of crown-dieback were categorized as "dieback" trees while, conversely, trees with healthy crowns or negligible amounts of crown dieback (e.g. some lateral branches had lost foliage) were categorized as "healthy" (Figure A-2). Each plot's central tree location was recorded using a GPS device and the remaining trees' locations were recorded relative to each plot's central tree, including distance and azimuth, by using a laser rangefinder/hypsometer and compass. Using these data, each tree's distance to the highway and other edge features were estimated in ArcMap using the Euclidean Distance tool.

Increment Core Collection, Preparation and Ring-width Analyses

We extracted three 12 mm increment cores at 1.3 m above the ground for each tree. In the laboratory, each core was mounted and sanded using 120-400 grit sandpaper. The cores were crossdated visually by identifying marker years from 1900-2018 (Yamaguchi, 1991). Ring widths were measured to the nearest 0.001 mm using a sliding stage (Velmex Inc. "TA system", Bloomfield, NY) and MeasureJ2X software (Voortech

Consulting). Crossdating was verified using the program COFECHA (Holmes, 1983) using a previously developed chronology from HRSP as a master chronology (Carroll et al., 2014; Voelker et al., 2018). Cores that contained >3 missing rings from 1900-2018 were excluded from analysis. Tree-ring statistics (Table 2) were calculated in R (R Core Team, 2018) using the package *dplR* (Bunn, 2008).

For the ring-width analyses, trees were grouped by edge type, i.e. road, secondary forest, agriculture, or control. Highway adjacent trees were split further based on crown health, crown dieback trees or healthy crowns and again, based on their proximity to the highway (<30 m or 30-160 m). Control trees were also analyzed separately by location, i.e. the Bull Creek area and the Pepperwood area, hereafter C1 and C2, respectively (Figure 2-1). In total, the tree-ring widths of eight groups of trees were used for all ring-width analyses.

To determine whether highway construction or other disturbances resulted in reduced radial growth, we used the disturbance detection method radial-growth averaging (Lorimer & Frelich, 1989; Nowacki & Abrams, 1997). Radial-growth averaging was selected because it is one of the more accurate disturbance detection methods while requiring little *a priori* knowledge (Trotsiuk et al., 2018). In this method, the growth change (%GC) for each year is calculated as a percentage by contrasting the average radial growth of a preceding window period, M_1 (including the target year) with average radial growth of a subsequent window period, M_2 (excluding the target year):

$$\%GC = \frac{M_2 - M_1}{M_1} * 100 \qquad \text{Equation 1}$$

Radial growth averaging was originally used to detect release events in understory trees by averaging radial growth over 15-year windows and using %GC thresholds of 50-

99% and >100% to categorize “moderate” and “major” releases, respectively (Lorimer & Frelich, 1989). This method was later modified using a 10-year window and a %GC threshold of ≥25% for moderate releases while keeping >100% %GC as the threshold for major releases to accommodate the different types of responses that were expected from canopy dominate trees in comparison to understory trees following disturbances (Nowacki & Abrams, 1997). Since then, there have been several adaptations to meet species-specific or site-specific criteria since the method is sensitive to parameter selection (Rubino & Mccarthy, 2004; Stan & Daniels, 2010). Shorter windows and lower thresholds increase the probability of false positives due to climatic variability, and longer windows and higher thresholds increase the probability of false negatives, so selection of these parameters should be done judiciously and based on the type of predicted response (Rubino & Mccarthy, 2004; Trotsiuk et al., 2018). We selected two sets of criteria to detect different suppression severities. To detect more ephemeral, moderate suppressions we used the parameters developed by Nowacki & Abrams (1997) (%GC threshold ≥25% and a 10-year window), however we adapted the %GC threshold to detect moderate suppressions, ≤ -25%, rather than moderate releases. Major suppressions that had a longer duration and a larger decrease in growth were detected using a 25-year window and a %GC threshold of ≤ -50%. Since this method uses moving windows and the last year of growth recorded was 2018, we could only detect growth suppressions until 2008 using the 10-year window and until 1993 using the 25-year window. It should also be noted that criteria for growth releases and growth suppressions represents different magnitudes of growth change. For growth releases, there is no strict limit on how fast trees can grow when released – values can be 200 or 300% or more.

However, for growth suppressions, growth can only decline until no annual growth is produced. Therefore, the %GC for detecting releases should always be greater compared to the detection of growth suppressions as shown by our major suppression criteria (50%) in comparison to major release criteria in other disturbances detection studies (e.g., ≥100% in Lorimer & Frelich, 1989; Nowacki & Abrams, 1997). Lastly, we required only one core from each tree to meet the %GC threshold in order to determine whether or not each tree was experiencing a growth suppression because *Cupressaceae* members often grow asymmetrically and growth responses to disturbance are often expressed on only one side of trees (Copenheaver et al., 2009). All radial growth averaging analyses were conducted using the *TRADER* package (Altman et al., 2014) in R (R Core Team, 2018).

Tree-ring Carbon Isotope Preparation and Analyses

To determine how proximity to a road impacted drought stress while accounting for climatic variation, we conducted dendroclimatic modeling of tree-ring carbon isotopes for trees adjacent to the highway with healthy and dieback crowns and for trees in our control groups. We selected two cores from trees that were missing ≤ 1 ring per core to conduct the carbon isotope analyses. The latewood of the tree rings from 1900-2017 was excised and pooled for stable carbon isotope analysis. Due to limitations in crossdating and coast redwoods' tendency to produce narrow rings and the difficulty of excising their latewood, group pooling was limited to six to ten trees. All samples were ground using a Wiley mill fitted with an 80-mesh screen, and ground wood particles were sealed in polypropylene mesh filter bags. Samples within filter bags were then bleached to α-cellulose using a sodium chlorite and glacial acetic acid solution followed by a sodium hydroxide solution and extensive rinsing in deionized water. Samples were

homogenized using an ultrasonic probe to break apart cellulose fibers and freeze dried (Laumer et al., 2009). All samples were weighed on a microbalance into tin capsules and their carbon isotope composition was measured at the Utah State University Stable Isotope Lab using standard high temperature combustion in a Costech 4010 Elemental Analyzer coupled to a Thermo Delta V AdVantage gas phase isotope ratio mass spectrometer.

All resulting $\delta^{13}C$ values reported here are expressed relative to the VPDB standard in ‰ where R is the ratio of ^{13}C to ^{12}C atoms of the sample or standard.

$$\delta^{13}C = \left(\frac{R_{sample}}{R_{standard}} - 1 \right) 1000 \qquad \text{(Equation 2)}$$

Due to atmospheric increases in $\delta^{13}CO_2$ as a result of fossil fuel burning, we converted all tree-ring $\delta^{13}C$ values to carbon discrimination values ($\Delta^{13}C$) following Farquhar, Ehleringer, and Hubick (1989):

$$\Delta^{13}C = (\delta^{13}C_A - \delta^{13}C_P) / (1 + \delta^{13}C_P/1000) \qquad \text{(Equation 3)}$$

Where $\delta^{13}C_P$ is the $\delta^{13}CO_2$ signature of the tree-rings, and $\delta^{13}C_A$ is the $\delta^{13}CO_2$ signature of air as represented by the values given in McCaroll and Loader (2004) merged with smoothed annual records from Mauna Loa, Hawaii (Keeling et al., 2005). Most variation in the carbon isotopic signature of sugar produced in leaves is driven by changes in stomatal conductance (Farquhar et al., 1989). When this signal is converted to $\Delta^{13}C$ of tree-rings, it largely reflects a canopy-integrated indicator of how stomata have responded to environmental stimuli such as drought stress, as modulated by leaf to air vapor pressure deficit (VPD) and soil moisture deficits (McCarroll & Loader, 2004). Thereby, we used tree-ring $\Delta^{13}C$ to assess the timing and duration of the highway's impact on

drought stress in old redwood trees, to the extent that this disturbance modulated canopy-integrated leaf gas exchange.

For dendroclimatic modeling, we trained linear regression models using the annual $\Delta^{13}C$ values for each group of trees and the principal components of monthly climate variables for the pre-construction period (1901-1955) and used those models to predict $\Delta^{13}C$ values for the full $\Delta^{13}C$ time series including the pre-construction (1901-1955) and post-construction period (1956-2017). After predicting $\Delta^{13}C$ values from 1901-2017, we tested for structural changes in the residuals to determine when each group deviated significantly from their corresponding climate model. We assume that since these models integrate the expected impact of influential climatic factors, differences between the model predictions and the observed values (i.e. residuals) should largely be due to non-climate factors such as disturbance.

The original $\Delta^{13}C$ values contained several additive outliers represented by individual annual spikes in $\Delta^{13}C$ in comparison to the surrounding values (Chen & Liu, 1993). Because these outliers represent individual peaks and do not represent step changes in $\Delta^{13}C$ values, they are likely due to sampling error and do not represent longer term changes in drought stress. Because these outliers decreased model fit and prediction power, they were removed, although similar structural changes in the residuals were observed when outliers were not removed. Outliers were detected and removed using the procedure outlined in Chen & Liu (1993) and implemented in the R package *tsoutliers* (López-de-Lacalle, 2019) (Figure A-3). The procedure reiteratively looped through each $\Delta^{13}C$ time series, detected outliers based on the residuals of a fitted ARIMA model, and adjusted the $\Delta^{13}C$ time series until outliers were no longer detected.

The adjusted $\Delta^{13}C$ values were fitted to linear regression models using the principal components of monthly climate variables. We conducted principal component analysis (PCA) on the climate variables to reduce collinearity and dimensionality in the climate variables while still capturing climatic variability. Climate variables that were used for PCA consisted of monthly Palmer Drought Severity Index (PDSI) data for California's North Coast Drainage Division (https://www.ncdc.noaa.gov/cag/divisional/time-series), 4 km gridded minimum and maximum VPD obtained from PRISM (Daly et al., 2008), and 4 km gridded precipitation, temperature (max, avg, and min), relative humidity (RH) and climatic moisture deficit (CMD) obtained from ClimateWNA (Wang et al., 2012). Climate data were obtained for each plot established at HRSP and then averaged together for PCA. A total of 108 principal components were produced following the PCA of the monthly climate data. We used a culminative variance threshold of 80% to select the number of principal components to serve as predictor variables for modeling as they accounted for a majority of climate variation while reducing the risk of overfitting. This threshold equated to the top 20 principal components being used for analysis. The selection of a culminative threshold is inherently arbitrary and other thresholds have been used in other studies (Jolliffe, 2006), however the selection of more components offered only nominal improvement in model performance while increasing the risk of overfitting.

To determine if and when the residuals for each group significantly deviated from their climate model, we used the R package *strucchange* (Zeileis et al., 2002, 2003) to identify structural changes in the residuals. This approach statistically detects changes in the mean of residuals. In this method, linear horizontal regression lines are fitted to the

residuals, and shift periods with different means are separated by breaks. The number of breaks in the residuals was determined using Bayesian Information Criterion (BIC) values provided by the function 'breakpoints' in *strucchange*.

Results

Crossdating

In total, 538 increment cores were extracted from 182 redwood trees. Of the cores extracted, ~55% were crossdated from 1900-2018 with ≤ 3 missing rings (Table 2-2). Generally, crossdating success was uniform across all groups, however highway adjacent trees with healthy crowns had much higher success rates. Healthy trees <30 m from the highway had a crossdating success rate of 71%, whereas 80% of healthy trees >30 m from the highway were crossdated successfully in comparison to the average of the other groups which was only 50%. Since tree-ring crossdating of redwoods has been historically difficult, we included tree-ring summary statistics for all groups that demonstrate our ability to effectively crossdate among cores within trees, among trees and among stands (Table 2-2). Specifically, the expressed population signal (EPS) was above a recommended threshold minimum of 0.85 (Cook & Kairiukstis, 1990; Wigley et al., 1984) for all groups. Effective chronology signal ($rbar_{eff}$) was highest for the control groups and trees neighboring secondary forest. $Rbar_{eff}$ was lowest in trees that neighbored agricultural areas.

Ring-width Analyses

Radial-growth averaging results revealed synchronous moderate growth suppressions between most groups, including control plots, during the early 1900s, 1920s, 1950s, 1990s, and late 2000s (Figure 2-2). The synchrony of these growth suppression patterns indicates similar environmental influences between groups, suggesting that the radial growth averaging methods should be robust to detect differences between groups, where they exist. Asynchronous patterns of moderate growth suppressions were found in dieback and healthy trees that were within 30 m of the highway (Figure 2-2A & Figure 2-2B). These two groups had the highest portion of trees, 73% and 90%, respectively, exhibiting a moderate growth suppression during the window of construction for the highway expansion, while healthy trees >30 m from the highway was the next closest group at 50%. Dieback trees <30 m of the highway was the only group to show signs of a major suppression in which 55% of those trees experienced a major suppression following the construction (Figure 2-3A). No tree from either control group experienced major growth suppressions, and <6% and 0% of trees bordering agricultural fields and secondary forests, respectively, exhibited a major growth suppression during the highway construction window. Besides the highway construction window, the other period where major suppressions were detected spanned 1900 until the mid-1920s for healthy and dieback trees as well as both control groups. C1 had the highest portion of trees that experienced a major suppression in that time window at 44% followed by C2 at 26% while the portion of healthy and dieback trees that experienced a major suppression ranged from 15% to 24%, respectively. Trees bordering agricultural

fields and secondary forests included 0% and 6.6% of trees that experienced a major suppression during the same window (Figure 2-3).

Carbon Isotope Analyses

On average, $\Delta^{13}C$ declined by ~2‰ across all groups between 1900 and 2017 regardless of outliers (Figure A-3). For most of the groups, a majority of the decline occurred early in the time series (~1900-1920), which corresponds to the period during and immediately after major growth suppressions were frequent across groups. Regression models trained using the climate principal components for the pre-construction period explained 56.74% and 43.26% of the variation in the adjusted $\Delta^{13}C$ values for dieback and healthy trees, respectively, and 66.03% and 57.36% of the variation for C1 and C2 trees, respectively. Residuals for diebacks trees were characterized by $\Delta^{13}C$ that was lower than expected from 1959-2005 (Figure 2-4A) whereas healthy trees exhibited values lower than expected from 1973-present (Figure 2-4B). In contrast $\Delta^{13}C$ of controls did not deviate from their predicted values during the window of construction. In fact, C1 did not significantly deviate from its predictions during the entire window of inquiry (Figure 2-4C) whereas C2 exhibited two significant shifts in 1994 and 2005 (Figure 2-4D).

Discussion

We assessed the effects that forest edges exert on tree-ring growth and carbon isotope composition of old redwoods. Our analyses provided support for the hypothesis that the construction of Highway 101 resulted in radial growth declines and elevated drought stress along the forest edge potentially contributing to the degradation of crown

health in these areas (Chapter 2). Declines in annual growth and elevated drought stress associated with highway construction occurred in trees with and without crown dieback and drought stress has lasted for ~50 years.

Crossdating

In this study, disturbance detection methods were employed using tree-ring data to quantify the impacts that the construction of Highway 101 had on redwoods in old-growth stands of HRSP. Similar to other attempts to crossdate coast redwoods (See Carroll et al., 2014, 2017), many cores exhibited ring attributes such as complacency, missing and wedging rings, spiral wood compression and false rings, that limited the number of cores that could be confidently crossdated and used for analyses. Accordingly, we were only able to crossdate ~55% of the cores across all groups from 1900-2018. Due to crossdating limitations and exclusion of cores due to missing rings, our results are likely conservative estimates of growth suppression and drought stress. It is likely that if a tree was impacted severely enough to restrict radial growth for several years, it would have been excluded from our analyses.

Overall, our crossdating success rate was lower than other redwood tree-ring studies that collected increment cores at multiple heights along the main trunk through the use of tree-climbing techniques (e.g. 82% in Carroll et al., 2014) or studies that were able to use full slabs of previously felled trees or stumps (Brown & Swetnam, 1994; Voelker et al., 2018). By collecting increment cores at various heights, the influence of the previously mentioned growth attributes can be minimized as these attributes are more prevalent at the lower base of the trunk (Carroll et al., 2014; Schulman, 1940). Similarly, the use of redwoods slabs allows one to follow multiple radii and avoid areas of wedging

and/or identify which rings are missing for higher crossdating accuracy (Brown & Swetnam, 1994; Voelker et al., 2018). While these techniques allow for higher crossdating accuracy, both techniques can be extremely labor-intensive and require specialized training (Carroll et al., 2017). Additionally, both rely on opportunistic sampling as not all trees are safe to climb and fallen redwoods from old-growth stands are rare and often not available for slab collection due to the desire of parks to protect the natural character of those forests.

The percentage of cores that we were able to confidently crossdate were comparable between most groups (Table 2-2), however both groups of highway adjacent trees with healthy crowns had notably higher proportions of their cores crossdated. This discrepancy between groups may be explained, partially, by differences in size and health status as both of these attributes make it increasingly likely that a redwood will have anomalous ring growth that will limit crossdating (Carroll et al., 2018b; Sillett et al., 2015). DBH values and tree heights of highway adjacent trees were smaller than the control trees and the other groups of trees that border secondary forest and agricultural areas (Table 2-1). This in part may explain the discrepancy in crossdating between the groups as tree ring wedging becomes more pervasive in larger trees. Additionally, while both DBH and height were comparable among healthy and dieback trees, the differences in crown vigor suggest that dieback trees were less healthy and therefore more prone to anomalous growth.

Tree Ring Analyses

To determine if the construction of the highway led to periods of growth suppression in trees that were adjacent to the highway, we used an adapted version of

radial growth averaging that has conventionally been used to identify the opposite pattern -- release events associated with past disturbances (Lorimer & Frelich, 1989; Nowacki & Abrams, 1997). By contrasting the patterns of growth suppression in plots that span the spatial extent of the park (Figure 2-1), we are inferring that synchronous suppression patterns are likely attributable to pressures that simultaneously impact all plots such as climate. The asynchronous suppression patterns should then highlight the differences in growth patterns that are likely driven by plot type. The levels of growth suppressions in trees near Highway 101 following its construction suggest that the previous highway expansion disproportionately impacted the radial growth of trees <30 m from the highway and was particularly impactful for trees with crown dieback. Similar growth suppression patterns have been observed in redwoods following known fire events (Carroll et al., 2018b), which may explain the suppression events we observed during the early 20th century (Figure 2-3) prior to organized fire suppression efforts in this region. The damage accrued during either a fire or road construction can result in suppression responses as trees are likely to experience restrictions in water and nutrient supply due to tissue damage. Trees may also redirect carbon and other resources to root and branch regeneration or reiteration via basal sprouting following disturbances events rather than investing resources into increment growth (Carroll et al., 2018b; Stoffel & Bollschweiler, 2008).

Our Δ13C modeling results suggest that, in combination with decreases in growth, redwoods with dieback in our study area experienced higher levels of drought stress than would be expected given the climatic conditions for almost 50 years. However, our results were not as consistent with healthy trees. This group observed a similar but

delayed response in drought stress, despite the radial averaging results suggesting that a large portion of these trees experienced a growth suppression immediately following the highway's construction (Figure 2-4). A possible explanation is that this discrepancy between our radial averaging results and $\Delta^{13}C$ residual breaks may be a result of different levels of damage between these two groups of trees. For healthy trees, it is possible that they underwent mild to moderate water restrictions that induced some moderate, but not a major growth suppression that did not result in crown dieback. This corresponded to only a mild reduction in both stomatal conductance and assimilation, and subsequently, no immediate changes in $\Delta^{13}C$. Conversely, dieback trees did undergo severe water restrictions that induced some moderate and severe growth suppressions in trees <30m. This caused dieback and reduced stomatal conductance relative to the rate of photosynthesis resulting in almost immediate decline in $\Delta^{13}C$. As dieback trees slowly recovered leaf area and competitive status after the abrupt dieback event, this increased stand-level competition for water resources which were likely altered due to soil compaction and water diversion as a result of the road which caused increasing stomatal closure in healthy trees after a 10 to 15-year lag.

Implications for Redwood Ecosystems

Land cover changes due to logging and conversions to residential areas, agricultural fields, and roads has left the remaining redwood forests heavily fragmented. The creation of abrupt, artificial forest boundaries has exposed the remaining trees to many different types of edge effects that can affect their ecological function significantly (Laurance et al., 2009; Laurance & Yensen, 1991; Russell et al., 2000). While our analyses show that trees within 30 m of Highway 101 were disproportionately affected by

its construction, our results do not indicate that impacts of the highway or other edge types cannot permeate beyond 30 m into old-growth redwood stands. The percentage of HE and DB trees that were >30 m from the highway and experienced a moderate growth suppression during the window of construction was more than double the average of our controls. Moreover, Russel et al. (2000) found that some edge effects can influence the conditions of an old-growth redwood forest >200 m into a forest interior. Given the proximity of the remaining redwood forests to artificial boundaries, it is estimated that ~40% of the redwood ecosystem, including secondary forest, experience edge effects (Burns et al., 2018).

The ecological effects of roads through fragmented forests is well documented (Goosem, 2007; Harper et al., 2005; Laurance et al., 2009; Trombulak & Frissell, 2000). By creating abrupt forest boundaries, roads can create areas with lasting legacies of elevated drought stress by increasing sunlight and wind exposure, and altering local hydrologic patterns. Indeed, roads have been found to contribute to sub-surface flow interception (Jones, 2000). In addition to how roads may elevate drought stress, increased wind exposure along forest edges have also been linked to increased windthrow events, and larger trees in particular, have been found to be more susceptible to these effects (Laurance & Curran, 2008). These findings are particularly concerning for redwoods considering they are the tallest species in the world and windthrow is one of the leading causes of mortality for these trees (Van Pelt et al., 2016). Roads and highways can also be large sources of chemical pollutants, such as dust, heavy metals, ozone and organic molecules, that lead to decreases in forest health and productivity (Laurance et al., 2009; Trombulak & Frissell, 2000). In addition to altering conditions of forest edges, roads also

provide increased access to forested areas that were previously inaccessible to humans, and in doing so, road expansions frequently led to increases in illegal exploitation of those areas. Although this type of exploitation is often described as increases in poaching and illegal mining, burl poaching is becoming increasingly more frequent in the Redwood National and State Parks and has been found to be closely associated with increased accessibility to roads (Kurland et al., 2018).

The extent to which edge effects impact fragmented forest is largely dependent on the characteristics of the forest edge. Areas in which multiple edges intersect forest boundaries are likely to experience elevated edge effects that permeate further into forest stands. Similarly, the shape of a stand can also influence the intensity of the edge effects. Small or irregularly shaped forest fragments that have high perimeter-to-area ratios are often more vulnerable to edge effects (Harris, 1984; Laurance & Yensen, 1991). Again, this may be problematic for redwoods as approximately half of all extant redwood old-growth stands have an area <30 acres (Burns et al., 2018). Additionally, the size of the road is often proportional to the intensity of the edge effects i.e. larger roads introduce edge effects that are more pervasive into stands than smaller roads (Laurance et al., 2007, 2009; Zhou et al., 2020), so while many roads within HRSP are narrow and may not have led to high rates of crown degradation, large roadways like Highway 101 are likely to introduce edge effects that are elevated relative to other narrower byways (Chapter 2). The restoration of secondary forest bordering remnant stands can help ameliorate many edge effects (Goosem, 2007; Laurance et al., 2009; Russell et al., 2000). However, for redwood ecosystems, a majority of the logged forest areas were harvested at least twice following Euro-American settlement, so only 2% of the remaining redwood

ecosystem is mature secondary redwood (Burns et al., 2018) which limits the areas in which secondary forest can buffer old-growth stands from edge effects.

Conclusion

As we enter an era of increasing infrastructure expansion and climatic uncertainty, it becomes increasingly important to evaluate the ecological consequences that human activity has on ecosystems, especially those as unique and iconic as the coast redwood forests that have already seen massive reductions despite a long history of conservation efforts. Redwoods have several traits that have made them relatively resilient against many types of disturbances such as fires and floods. However, their shallow root system, lack of soil water uptake efficiency, and extreme height appear to make these trees, particularly the larger trees, vulnerable to dieback and crown deterioration when novel levels of drought stress are incurred. The fragmentation of remaining old-growth stands and a lack of mature secondary forest that could help buffer edge-effects suggest that, in its current state, the redwood ecosystem is highly susceptible to the deleterious effects of additional abrupt forest edges and other activities that may alter hillslope hydrology. Despite the rarity of old-growth redwood forest and their biological and cultural significance, very few studies (Russell et al., 2000) have directly investigated the implications that artificial forest edges have on old-growth redwood forests' ecological function. The findings presented here provide an incremental step toward quantifying the impacts of forest edges and highway construction disturbance on coast redwoods, but further research may be warranted to elucidate how these findings may apply in different climatological settings and whether more detailed spatial analyses would reveal that road

and forest edge arrangements are particularly likely to cause drought stress and crown dieback in large trees.

References

Altman, J., Fibich, P., Dolezal, J., & Aakala, T. (2014). TRADER: A package for Tree Ring Analysis of Disturbance Events in R. *Dendrochronologia*, *32*, 107–112. https://doi.org/10.1016/j.dendro.2014.01.004

Brown, P., & Swetnam, T. (1994). A cross-dated fire history from coast redwood near Redwood National Park, California. *Canadian Journal of Forest Research*, *24*, 21–31. https://doi.org/10.1139/x94-004

Bunn, A. G. (2008). A dendrochronology program library in R (dplR). *Dendrochronologia*, *26*(2), 115–124. https://doi.org/10.1016/j.dendro.2008.01.002

Burgess, S., & Dawson, T. E. (2004). The contribution of fog to the water relations of Sequoia sempervirens (D. Don): Foliar uptake and prevention of dehydration. *Plant, Cell and Environment*, *27*, 1023–1034. https://doi.org/10.1111/j.1365-3040.2004.01207.x

Burns, E. E., Campbell, R., & Cowan, P. D. (2018). *State of Redwoods Conservation Report: A Tale of Two Forests*. https://www.savetheredwoods.org/wp-content/uploads/State-of-Redwoods-Conservation-Report-Final-web.pdf

California State Parks. (n.d.). *About Coast Redwoods*. https://www.parks.ca.gov/?page_id=22257

Carroll, A. L., Sillett, S. C., Coonen, E. J., & Iberle, B. G. (2017). Expanding the Network of Crossdated Tree-ring Chronologies for Sequoia sempervirens.

Proceedings of the Coast Redwood Science Symposium, 25–33.

Carroll, A. L., Sillett, S. C., & Kramer, R. D. (2014). Millennium-scale crossdating and inter-annual climate sensitivities of standing California redwoods. *PLoS ONE*, *9*(7). https://doi.org/10.1371/journal.pone.0102545

Carroll, A. L., Sillett, S. C., Palladini, M., & Campbell-Spickler, J. (2018a). Dendrochronological analysis of Sequoia sempervirens in an interior old-growth forest. *Dendrochronologia*, *52*, 29–39. https://doi.org/10.1016/j.dendro.2018.09.006

Carroll, A. L., Sillett, S. C., & Van Pelt, R. (2018b). Tree-Ring Indicators of Fire in Two Old-Growth Coast Redwood Forests. *Fire Ecology*, *14*(1), 85–105. https://doi.org/10.4996/fireecology.140185105

Chen, C., & Liu, L.-M. (1993). Joint Estimation of Model Parameters and Outlier Effects in Time Series. *Journal of the American Statistical Association*, *88*(421), 284–297. https://doi.org/10.2307/2290724

Cook, Edward R. (1987). The Decomposition of Tree-Ring Series for Environmental Studies. *Tree-Ring Bulletin*, *47*, 37–59. https://doi.org/S

Cook, Edward R., & Kairiukstis, L. (1990). *Methods of Dendrochronology: Applications in the Environmental Sciences* (E. R. Cook & L. A. Kairiukstis (eds.)). Kluwer Academic Publishers. https://doi.org/10.1007/978-94-015-7879-0

Copenheaver, C. A., Black, B. A., Stine, M. B., McManamay, R. H., & Bartens, J. (2009). Identifying dendroecological growth releases in American beech, jack pine, and white oak: Within-tree sampling strategy. *Forest Ecology and Management*, *257*, 2235–2240. https://doi.org/10.1016/j.foreco.2009.02.031

Daly, C., Halbleib, M., Smith, J. I., Gibson, W. P., Doggett, M. K., Taylor, G. H., Curtis, J., & Pasteris, P. P. (2008). Physiographically sensitive mapping of climatological temperature and precipitation across the conterminous United States. *International Journal of Climatology*, *28*(15), 2031–2064. https://doi.org/10.1002/joc.1688

Dawson, T. E. (1998). Fog in the California redwood forest: ecosystem inputs and use by plants. *Oecologia*, *117*, 476–485.

Domec, J. C., Schäfer, K., Oren, R., Kim, H. S., & McCarthy, H. R. (2010). Variable conductivity and embolism in roots and branches of four contrasting tree species and their impacts on whole-plant hydraulic performance under future atmospheric CO2 concentration. *Tree Physiology*, *30*(8), 1001–1015. https://doi.org/10.1093/treephys/tpq054

Farquhar, G. D., Ehleringer, J. R., & Hubick, K. T. (1989). Carbon Isotope Discrimination and Photosynthesis. *Annual Review of Plant Physiology and Plant Molecular Biology*, *40*(1), 503–537. https://doi.org/10.1146/annurev.pp.40.060189.002443

Fritts, H. C. (1976). *Tree Rings and Climate*. Elsevier. https://doi.org/10.1016/B978-0-12-268450-0.X5001-0

Fritz, E. (1929). Some popular fallacies concerning California redwood. *Madroño 1*, 221–224.

Fritz, E. (1932). The role of fire in the redwood region. *University of California Agricultural Experiment Station Circular*, 323.

Gessler, A., Cailleret, M., Joseph, J., Schönbeck, L., Schaub, M., Lehmann, M., Treydte,

K., Rigling, A., Timofeeva, G., & Saurer, M. (2018). Drought induced tree mortality - a tree-ring isotope based conceptual model to assess mechanisms and predispositions. *New Phytologist*, *219*(2), 485–490. https://doi.org/10.1111/nph.15154

Goosem, M. (2007). Fragmentation impacts caused by roads through rainforests. *Current Science*, *93*(11), 1587–1595.

Harper, K. A., Macdonald, S. E., Burton, P. J., Chen, J., Brosofske, K. D., Saunders, S. C., Euskirchen, E. S., Roberts, D., Jaiteh, M. S., & Esseen, P.-A. (2005). Edge Influence on Forest Structure and Composition in Fragmented Landscapes. *Conservation Biology*, *19*(3), 768–782. https://doi.org/10.1111/j.1523-1739.2005.00045.x

Harris, L. D. (1984). *The fragmented forest: Island biogeography theory an the preservation of biotic diversity.* University of Chicago Press.

Holmes, R. L. (1983). Computer-Assisted Quality Control in Tree-Ring Dating and Measurement. In *Tree-Ring Bulletin*. Tree-Ring Society. http://hdl.handle.net/10150/261223

Johnstone, J. A., & Dawson, T. E. (2010). Climatic context and ecological implications of summer fog decline in the coast redwood region. *Proceedings of the National Academy of Sciences of the United States of America*, *107*(10), 4533–4538. https://doi.org/10.1073/pnas.0915062107

Johnstone, J. A., Roden, J. S., & Dawson, T. E. (2013). Oxygen and carbon stable isotopes in coast redwood tree rings respond to spring and summer climate signals. *Journal of Geophysical Research: Biogeosciences*, *118*(4), 1438–1450.

https://doi.org/10.1002/jgrg.20111

Jolliffe, I. T. (2006). Choosing a Subset of Principal Components or Variables. In *Principal Component Analysis* (pp. 111–149). Springer-Verlag. https://doi.org/10.1007/0-387-22440-8_6

Jones, J. A. (2000). Hydrologic processes and peak discharge response to forest removal, regrowth, and roads in 10 small experimental basins, Western Cascades, Oregon. *Water Resources Research*, *36*(9), 2621–2642. https://doi.org/10.1029/2000WR900105

Koch, G. W., Stillet, S. C., Jennings, G. M., & Davis, S. D. (2004). The limits to tree height. *Nature*, *428*(6985), 851–854. https://doi.org/10.1038/nature02417

Kurland, J., Pires, S. F., & Marteache, N. (2018). The spatial pattern of redwood burl poaching and implications for prevention. *Forest Policy and Economics*, *94*, 46–54. https://doi.org/10.1016/j.forpol.2018.06.009

Laumer, W., Andreu, L., Helle, G., Schleser, G. H., Wieloch, T., & Wissel, H. (2009). A novel approach for the homogenization of cellulose to use micro-amounts for stable isotope analyses. *Rapid Communications in Mass Spectrometry*, 1934–1940. https://doi.org/10.1002/rcm

Laurance, W. F., & Curran, T. J. (2008). Impacts of wind disturbance on fragmented tropical forests: A review and synthesis. *Austral Ecology*, *33*, 399–408. https://doi.org/10.1111/j.1442-9993.2008.01895.x

Laurance, W. F., Goosem, M., & Laurance, S. G. W. (2009). Impacts of roads and linear clearings on tropical forests. *Trends in Ecology and Evolution*, *24*(12), 659–669. https://doi.org/10.1016/j.tree.2009.06.009

Laurance, W. F., Nascimento, H. E. M., Laurance, S. G., Andrade, A., Ewers, R. M., Harms, K. E., Luizão, R. C. C., & Ribeiro, J. E. (2007). Habitat fragmentation, variable edge effects, and the landscape-divergence hypothesis. *PLoS ONE*, *2*(10). https://doi.org/10.1371/journal.pone.0001017

Laurance, W. F., & Yensen, E. (1991). Predicting the impacts of edge effects in fragmented habitats. *Biological Conservation*, *55*, 77–92. https://doi.org/https://doi.org/10.1016/0006-3207(91)90006-U

Lee, C. A., & Muzika, R.-M. (2014). Plant senescence for ecologists : precision in concept , scale , and terminology. *Plant Ecology*, *215*, 1417–1422. https://doi.org/10.1007/s11258-014-0398-8

López-de-Lacalle, J. (2019). *tsoutliers: Detection of Outliers in Time Series*. https://cran.r-project.org/package=tsoutliers

Lorimer, C. G., & Frelich, L. E. (1989). A methodology for estimating canopy disturbance frequency and intensity in dense temperate forests. *Canadian Journal of Forest Research*, *19*(5), 651–663. https://doi.org/10.1139/x89-102

Lorimer, C. G., Porter, D. J., Madej, M. A., Stuart, J. D., Veirs, S. D., Norman, S. P., O'Hara, K. L., & Libby, W. J. (2009). Presettlement and modern disturbance regimes in coast redwood forests: Implications for the conservation of old-growth stands. *Forest Ecology and Management*, *258*(7), 1038–1054. https://doi.org/10.1016/j.foreco.2009.07.008

Madej, M. A. (2010). Redwoods, restoration, and implications for carbon budgets. *Geomorphology*, *116*, 264–273. https://doi.org/10.1016/j.geomorph.2009.11.012

McCarroll, D., & Loader, N. J. (2004). Stable isotopes in tree rings. *Quaternary Science*

Reviews, *23*, 771–801. https://doi.org/10.1016/j.quascirev.2003.06.017

Noss, R. (2000). The Redwood Forest: History, Ecology, and Conservation of the Coast Redwoods. *Bibliovault OAI Repository, the University of Chicago Press*.

Nowacki, G. J., & Abrams, M. D. (1997). Radial-growth averaging criteria for reconstructing disturbance histories fro ... *Ecological Monographs*, *67*(2), 225–234.

Olson, D. F., Douglass, R. F., & Walters, G. A. (1990). Sequoia sempervirens. *In Silvics of North America, Volume 1, Conifers. USDA Forest Service Handbook*, 654.

R Core Team. (2018). *R: A Language and Environment for Statistical Computing*. https://www.r-project.org/

Robinson, J. (1964). The Redwood Highway-Part III. *California Highways and Public Works*, *43*(Sep-Oct), 14–24.

Roden, J. S., Johnstone, J. A., & Dawson, T. E. (2009). Intra-annual variation in the stable oxygen and carbon isotope ratios of cellulose in tree rings of coast redwood (Sequoia sempervirens). *Holocene*, *19*(2), 189–197. https://doi.org/10.1177/0959683608098959

Roden, J. S., Johnstone, J. A., & Dawson, T. E. (2011). Regional And Watershed-Scale Coherence In the Stable-Oxygen and Carbon Isotope Ratio Time Series In Tree Rings Of Coast Redwood (Sequoia sempervirens). *Tree-Ring Research*, *67*(2), 71–86. https://doi.org/10.3959/2010-4.1

Rubino, D. L., & Mccarthy, B. C. (2004). Comparative analysis of dendroecological methods used to assess disturbance events. *Dendrochronologia*, *3*, 97–115.

Russell, W. H., McBride, J. R., & Carnell, K. (2000). Edge effects and the effective size

of old-growth coast redwood preserves. *Proceedings Rocky Mountain Research Station, USDA Forest Service*, *3*, 128–136. https://www.fs.usda.gov/treesearch/pubs/21978

Schulman, E. (1940). Climatic chronology in some coast redwoods. *Tree-Ring Bulletin*, *6*, 22–23.

Sillett, S. C., & Van Pelt, R. (2000). Tree Whose Crown is a Forest Canopy. *Northwest Science*, *74*(1), 34–43.

Sillett, S. C., Van Pelt, R., Carroll, A. L., Kramer, R. D., Ambrose, A. R., & Trask, D. (2015). How do tree structure and old age affect growth potential of california redwoods? *Ecological Monographs*, *85*(2), 181–212. https://doi.org/10.1890/14-1016.1

Smith, D. M. (1986). *The Practice of Silviculture*. John Wiley and Sons, Inc.

Stan, A. B., & Daniels, L. D. (2010). Calibrating the radial-growth averaging method for detecting releases in old-growth forests of coastal British Columbia, Canada. *Dendrochronologia*, *28*(3), 135–147. https://doi.org/10.1016/j.dendro.2009.10.003

Stoffel, M., & Bollschweiler, M. (2008). Tree-ring analysis in natural hazards research - An overview. *Natural Hazards and Earth System Science*, *8*(2), 187–202. https://doi.org/10.5194/nhess-8-187-2008

Stone, E. C., & Vasey, R. B. (1968). Preservation Of Coast Redwood on Alluvial Flats. *Science*, *159*(3811), 157–161.

Trombulak, S. C., & Frissell, C. A. (2000). Review of ecological effects of roads on terrestrial and aquatic communities. *Conservation Biology*, *14*(1), 18–30.

https://doi.org/10.1046/j.1523-1739.2000.99084.x

Trotsiuk, V., Pederson, N., Druckenbrod, D. L., Orwig, D. A., Bishop, D. A., Barker-Plotkin, A., Fraver, S., & Martin-Benito, D. (2018). Testing the efficacy of tree-ring methods for detecting past disturbances. *Forest Ecology and Management*, *425*, 59–67. https://doi.org/10.1016/j.foreco.2018.05.045

Van Pelt, R., Sillett, S. C., Kruse, W. A., Freund, J. A., & Kramer, R. D. (2016). Emergent crowns and light-use complementarity lead to global maximum biomass and leaf area in Sequoia sempervirens forests. *Forest Ecology and Management*, *375*, 279–308. https://doi.org/10.1016/j.foreco.2016.05.018

Voelker, S. L., Muzika, R.-M., & Guyette, R. P. (2008). Individual Tree and Stand Level Influences on the Growth, Vigor, and Decline of Red Oaks in the Ozarks. *Forest Science*, *54*(1), 8–20. https://doi.org/10.1093/forestscience/54.1.8

Voelker, S. L., Roden, J. S., & Dawson, T. E. (2018). Millennial-scale tree-ring isotope chronologies from coast redwoods provide insights on controls over California hydroclimate variability. *Oecologia*, *187*(4), 897–909. https://doi.org/10.1007/s00442-018-4193-4

Voelker, S. L., Merschel, A. G., Meinzer, F. C., Ulrich, D. E. M., Spies, T. A., & Still, C. J. (2019). Fire deficits have increased drought sensitivity in dry conifer forests: Fire frequency and tree-ring carbon isotope evidence from Central Oregon. *Global Change Biology*, *August 2018*, 1–16. https://doi.org/10.1111/gcb.14543

Wang, T., Hamann, A., Spittlehouse, D. L., & Murdock, T. Q. (2012). ClimateWNA-high-resolution spatial climate data for western North America. *Journal of Applied Meteorology and Climatology*, *51*(1), 16–29.

https://doi.org/10.1175/JAMC-D-11-043.1

Wigley, T. M. L., Briffa, K. R., & Jones, P. D. (1984). On the average value of correlated time series with applications in dendroclimatology and hydrometeorology. *Journal of Climate & Applied Meteorology*. https://doi.org/10.1175/1520-0450(1984)023<0201:OTAVOC>2.0.CO;2

Yamaguchi, D. (1991). A simple method for cross-dating increment cores from living trees. *Canadian Journal of Forest Research*, *21*(3), 414–416.

Zarnoch, S. J., Bechtold, W. A., & Stolte, K. W. (2004). Using crown condition variables as indicators of forest health. *Canadian Journal of Forest Research*, *34*(5), 1057–1070. https://doi.org/10.1139/x03-277

Zeileis, A., Kleiber, C., Krämer, W., & Hornik, K. (2003). Testing and Dating of Structural Changes in Practice. *Computational Statistics & Data Analysis*, *44*, 109–123.

Zeileis, A., Leisch, F., Hornik, K., & Kleiber, C. (2002). strucchange: An R Package for Testing for Structural Change in Linear Regression Models. *Journal of Statistical Software, Articles*, *7*(2), 1–38. https://doi.org/10.18637/jss.v007.i02

Zhou, T., Luo, X., Hou, Y., Xiang, Y., & Peng, S. (2020). Quantifying the effects of road width on roadside vegetation and soil conditions in forests. *Landscape Ecology*, *35*, 69–81. https://doi.org/10.1007/s10980-019-00930-8

Tables and Figures

Table 2-1: Tree size and crown characteristics among and between groups (±SE). Groups denoted <30 m (0 to 30) and >30 m (30 to 160) represent distance values in meters from California State Highway 101.

Identification	DBH (m)		Maximum Height (m)		Crown Dieback (%)		Crown Volume (m^3)		Crown Volume / Basal Area (m)	
Dieback <30 m	226	(±12)	65	(±2)	13	(±3)	5192	(±688)	1296	(±130)
Dieback >30 m	253	(±11)	76	(±2)	17	(±2)	9833	(±1281)	2039	(±284)
Healthy <30 m	157	(±5)	62	(±3)	0	(±)	5126	(±652)	2633	(±373)
Healthy >30 m	209	(±9)	71	(±1)	0	(±)	8458	(±837)	2590	(±229)
Bull Creek (C1)	324	(±23)	92	(±2)	1	(±1)	13,532	(±1977)	1552	(±120)
Pepperwood (C2)	284	(±18)	88	(±2)	1	(±)	13994	(±1508)	2402	(±247)
Secondary Forest	275	(±15)	86	(±2)	0	(±)	15,484	(±2319)	2548	(±309)
Agriculture	225	(±12)	77	(±3)	1	(±1)	6980	(±676)	1838	(±204)

Table 2-2: Tree-ring statistics for each group.

[a] Average number of trees from 1900-2018

[b] Mean correlation between different cores

[c] Mean within tree correlations

[d] Mean between tree correlations

ID	Crossdated cores (n)	Crossdated trees (n)	Average trees (n)[a]	Rbar tot[b]	Rbar wt[c]	Rbar bt[d]	Rbar eff[e]	EPS[f]	SNR[g]	Interseries correlation	Cores crossdated (%)
Dieback <30 m	23	11	10.95	0.364	0.689	0.344	0.401	0.88	7.315	0.510	55.56
Dieback >30 m	36	20	18.067	0.266	0.431	0.26	0.314	0.892	8.269	0.513	50.60
Healthy <30 m	22	10	9.739	0.429	0.588	0.416	0.506	0.909	9.996	0.569	70.97
Healthy >30 m	96	39	38.521	0.388	0.55	0.385	0.511	0.976	40.324	0.558	80.45
Bull Creek (C1)	32	16	15.966	0.479	0.555	0.476	0.584	0.957	22.452	0.506	50.00
Pepperwood (C2)	31	18	17.908	0.43	0.421	0.431	0.53	0.953	20.197	0.419	49.21
Agriculture	30	16	15.95	0.242	0.453	0.233	0.285	0.864	6.344	0.415	50.00
Secondary Forest	27	14	13.966	0.465	0.622	0.457	0.531	0.941	15.836	0.393	45.76

[e] Effective chronology signal

[f] Expressed population signal

[g] Signal to noise ratio

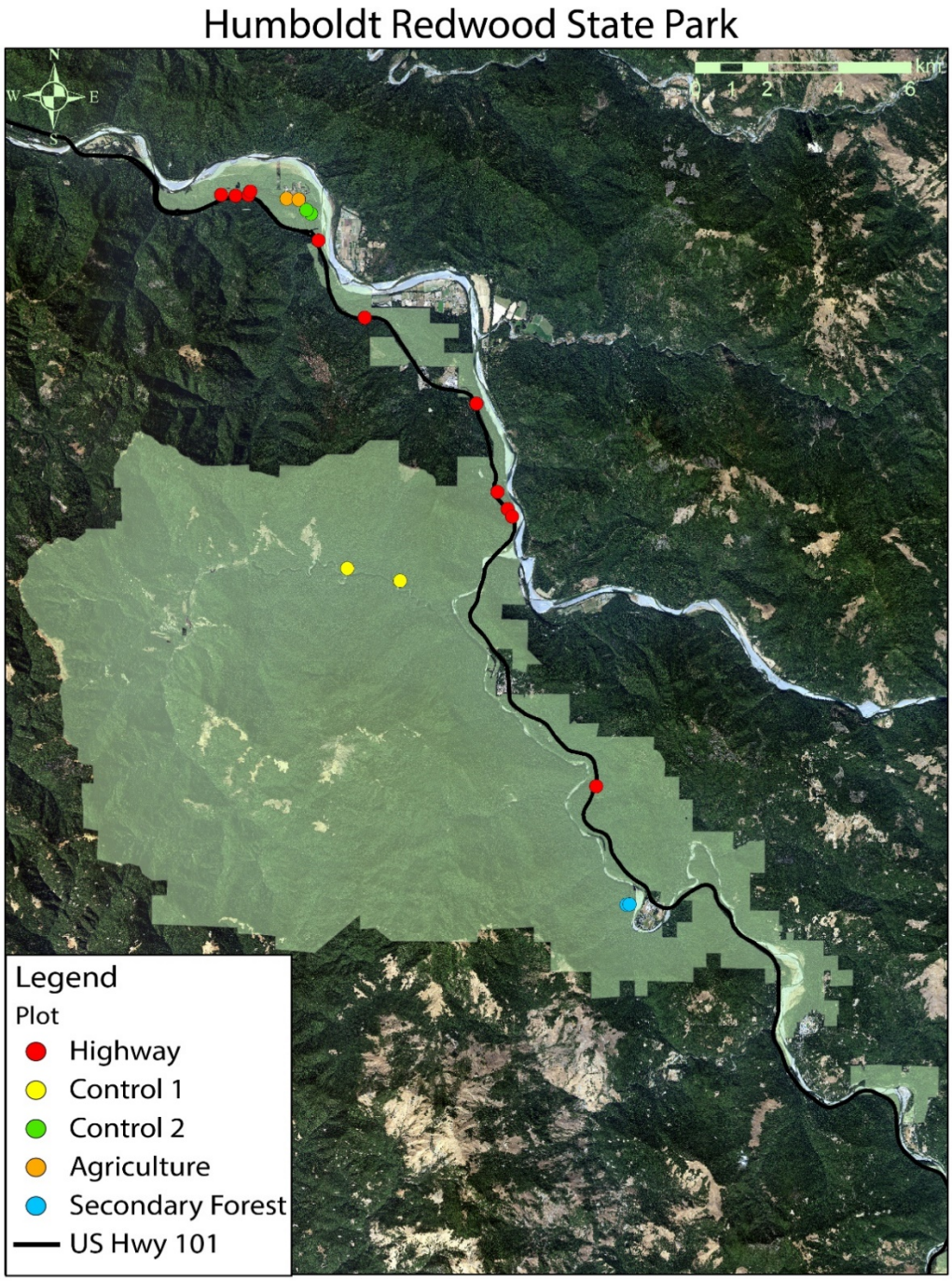

Figure 2-1: Plot locations within Humboldt Redwoods State Park. Red dots represent plots adjacent to Highway 101. Orange and blue dots represent plots established adjacent to non-road disturbance areas. Yellow and green dots represent reference stands established near Bull Creek in the Rockefeller forest (yellow) and near Pepperwood, CA (green). Figure adapted from Carroll et al. 2014.

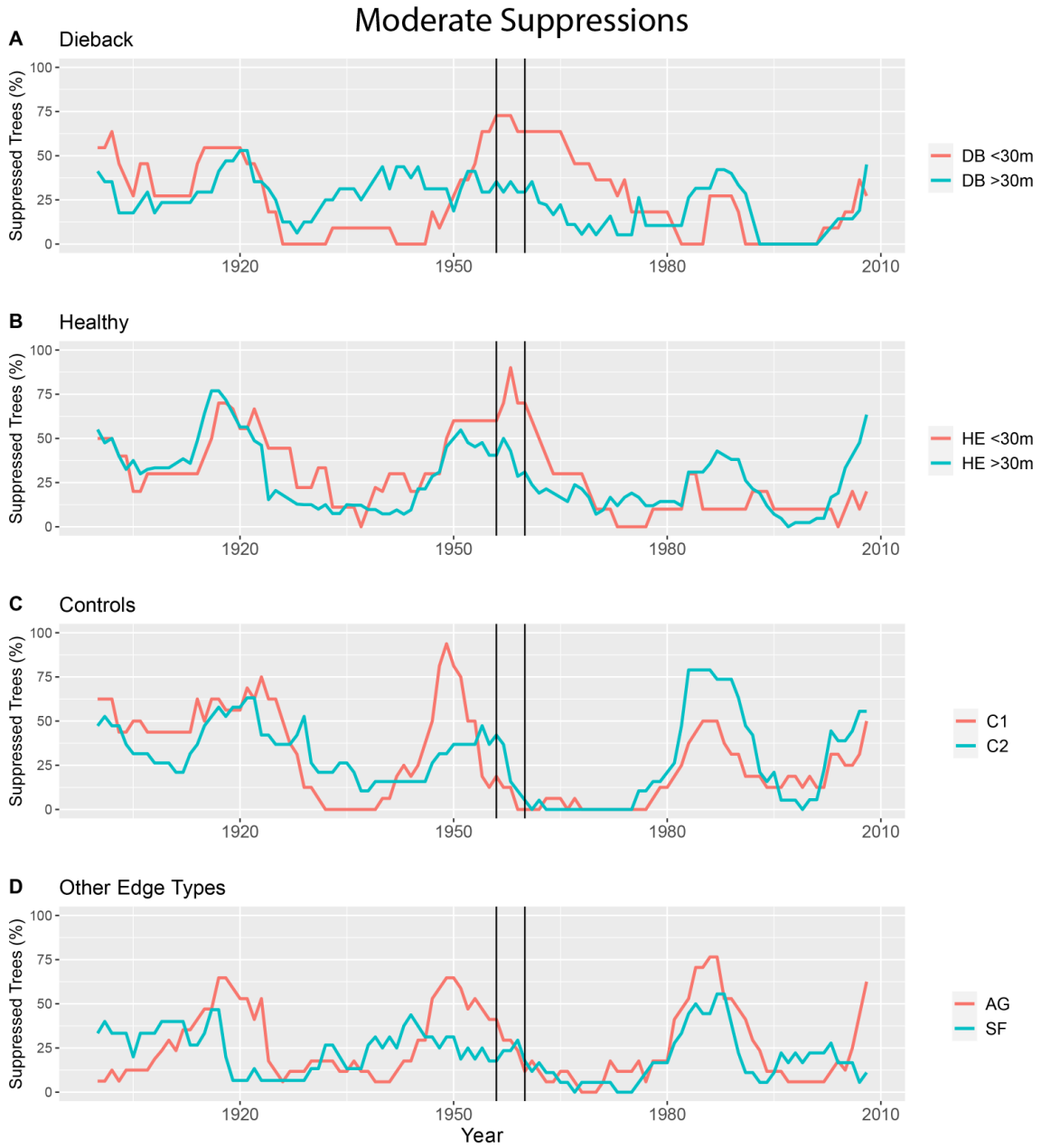

Figure 2-2: Radial growth averaging results showing the percentage of trees experiencing moderate growth suppressions from 1900-2008. Moderate growth suppressions were defined as growth changes ≤ -25% over a 10-year window. Black vertical lines mark the first and last year of road construction 1956-1960. (A) Dieback trees within 30 m of the highway (red line; DB <30 m) and dieback trees farther than 30 m from the highway (blue line; DB >30 m). Similarly, Healthy trees within 30 m of the highway (red line; HE <30 m) and dieback trees farther than 30 m from the highway (blue line; HE >30 m). (C) Control trees located near Bull Creek (red line; C1) in the Rockefeller forest and control trees located near Pepperwood, CA (blue line; C2). (D) Trees neighboring other agricultural fields (red line; AG) and secondary forest (blue line; SF).

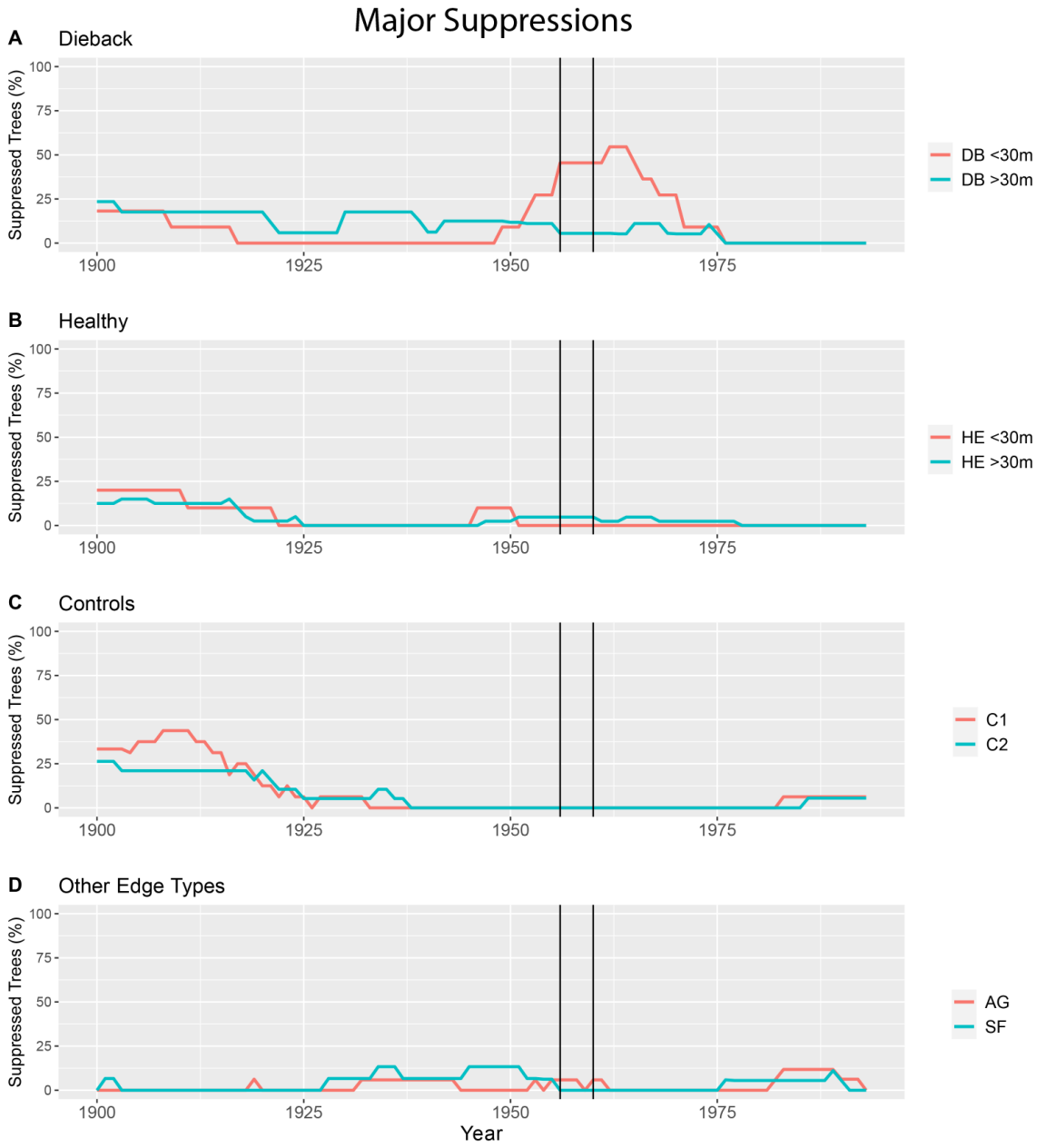

Figure 2-3: Radial growth averaging results showing the percentage of trees experiencing major growth suppressions from 1900-1993. Major growth suppressions were defined as growth changes ≤ -50% over a 25-year window. Black vertical lines mark the first and last year of road construction 1956-1960. (A) Dieback trees within 30 m of the highway (red line; DB <30 m) and dieback trees farther than 30 m from the highway (blue line; DB >30 m). Similarly, Healthy trees within 30 m of the highway (red line; HE <30 m) and dieback trees farther than 30 m from the highway (blue line; HE >30 m). (C) Control trees located near Bull Creek (red line; C1) in the Rockefeller forest and control trees located near Pepperwood, CA (blue line; C2). (D) Trees neighboring other agricultural fields (red line; AG) and secondary forest (blue line; SF).

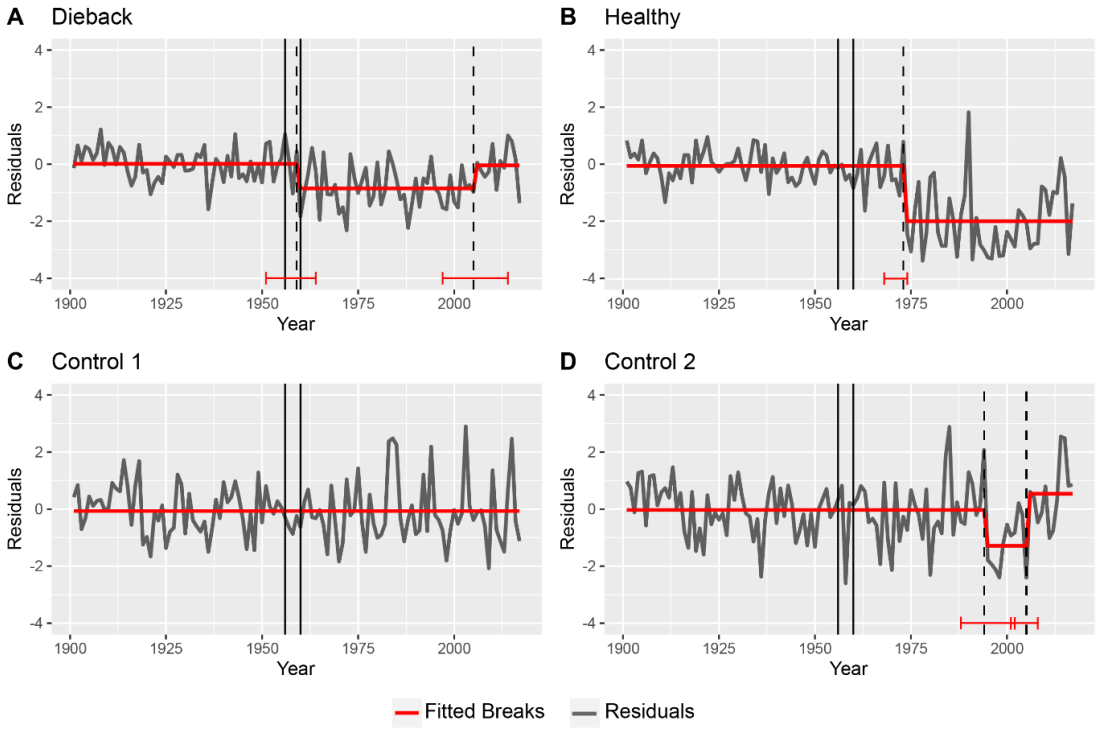

Figure 2-4: Break points of climate model residuals. Shown in each plot are residual values (grey lines) for each climatic model, fitted regression lines of linear models representing shifts in the residuals (red lines), and the confidence intervals for the timing of each shift (red error bars). Black vertical lines mark the first and last year of road construction 1956-1960. Dotted vertical lines mark the year of each shift. (A) Dieback trees adjacent to the road. (B) Healthy trees adjacent to the road. (C) Control trees located near Bull Creek in the Rockefeller forest. (D) Control trees located near Pepperwood, CA.

CHAPTER 3

INTEGRATING AERIAL IMAGERY AND LIDAR DATA TO QUANTIFY CROWN DETERIORATION IN HUMBOLDT REDWOOD STATE PARK

Abstract

While the impressive stature of coast redwood (*Sequoia sempervirens*) old-growth forests is both ecologically and culturally valuable, their extreme height and density has also limited the use of traditional ground-based methods for assessing forest health at large spatial scales. Fortunately, in recent decades, the increasing accessibility and resolution of publicly available remote sensing data has provided a viable avenue for conducting cost-efficient forest health assessments. In this study, we integrated classifications of National Agriculture Imagery Program (NAIP) with individual tree extents derived from discrete return Light Detection and Ranging (LiDAR) data to map the prevalence of crown dieback in Humboldt Redwood State Park (HRSP). We also examined different environmental variables including proximity to forest edge and topography as well as local tree density and height to investigate potential drivers of crown dieback. Using these methods, individual crown health was identified at 94% accuracy rate. Our crown health maps showed that crown dieback was relatively rare across a large majority of the park, however it was also heavily concentrated in the northern portion of the park where it aggregated near roads and previously clearcut areas. Tree height was the most important variable for discerning crown health and was consistently higher in trees with crown dieback than trees with healthy crowns. The findings of this study are consistent with previous literature that have shown taller trees have higher risk of hydraulic failure and partial dieback. Collectively, our results suggest

that the constraints that tree height places on maintaining healthy water column can also compound with the desiccation effects of forest edges which may led to elevated rates of crown dieback. Our results also show that publicly available remote sensing data can be a viable methodology for to detecting the health status of individual redwoods at high accuracy and may be useful for future assessments.

Introduction

Since Euro-American settlement, the majority of old-growth coast redwood (*Sequoia sempervirens*) forest has been lost due to extensive logging and land cover changes to roads, agricultural fields, and residential and urban areas. Today, only 5% of old-growth redwood forest remain, often standing in isolated patches with <30 acres (Burns et al., 2018). These remnant old-growth stands host the tallest trees in the world which can attain ages >2,000 years and hold the largest concentration of above-ground carbon per acre globally (Van Pelt et al., 2016). The extreme height and fragmentated nature of these stands adjacent to areas that were previously clear cut or converted to other land cover types creates abrupt transitions with stark height differences between intact forest and the surrounding areas. These forest edges expose the remaining trees to elevated sunlight and wind intensities, potentially increasing their drought stress and susceptibility to crown dieback and mortality (Laurance et al., 2007; Russell et al., 2000). While preservation efforts have helped retain large portions of the remaining old-growth redwood forest, edge effects continue to be major stressors in the redwood ecosystem and threaten to compound with anthropogenic climate change to further contribute to redwood forest degradation (Burns et al., 2018; Fernández et al., 2015; Johnstone & Dawson, 2010).

Prior to Euro-American settlement, the largest constraint on the extent of the redwood species was the presence or absence of a stable mesic climate (Noss, 2000). The current distribution of redwoods is considered a relic of a much larger historic distribution that receded to the coasts of California and Oregon following global cooling and drying climatic shifts (Johnstone & Dawson, 2010; Pittermann et al., 2012). Coastal upwelling and fog inundation have provided the hydrologic conditions necessary for the continued persistence of redwoods in its current range (McLaughlin et al., 2017). Redwoods' reliance on a mesic climate can be attributed, at least partially, to an aggregation of traits that considerably reduce its resistance to drought. Despite their extreme height, redwoods have relatively shallow root system and lack of roots hairs which limits their access and uptake efficiency of deep groundwater sources (Burgess & Dawson, 2004; Fritz, 1929; Olson et al., 1990; Stone & Vasey, 1968). Instead, they have been shown to have a greater reliance on shallow subsurface water from fog interception and fog drip during dry summer months and periods of drought (Burgess & Dawson, 2004; Dawson, 1998; Johnstone et al., 2013; Roden et al., 2009). Dawson (1998) found that the water derived from fog can attribute upwards of 40% of the water used during transpiration. Furthermore, the coast redwood is also a relatively anisohydric species in comparison to its more drought resistant relative, the giant sequoia (*Sequoiadendron giganteum*) and has been found to lack stomatal control during periods of elevated drought stress increasing their susceptibility to hydraulic failure which can lead to partial crown dieback or mortality (Ambrose et al., 2015).

The near-coastal zone of Northern California has provided a stable climate for redwoods and has long served as a hydrologic refugium during some of the most severe

droughts of the last 1000 years (Voelker et al., 2018). However, recent studies have also suggested that the frequency of fog inundation has declined ~33% since 1900 (Johnstone & Dawson, 2010) and projections of the species' future distribution predicts a 50% range contraction in the southern and central range of the species, particularly along the eastern edge of the distribution, by 2030 (Fernández et al., 2015). As decreases in precipitation continue to cause widespread elevated rates of tree mortality in many species (Allen et al., 2010) and climatic forecasts suggest large reductions in the redwood distribution (Fernández et al., 2015), it becomes increasingly important to investigate how human activity and habitat fragmentation affect the crown health and structure of the remaining old-growth redwood forests.

Limited crown visibility in old-growth redwoods due to their height and density has made it difficult to conduct ecological assessments on redwoods. Obtaining reliable data for ground-based metrics such as annual ring widths via increment core extraction (Chapter 1) or diameter at breast height (DBH) (Sillett et al., 2015) can also be complicated due to extensive buttressing at the lower portions of the trunk in mature redwoods. To circumvent these challenges many studies have employed tree climbing methods to gain access into the canopy (Ambrose et al., 2009; Carroll et al., 2014, 2018; Koch et al., 2004; Sillett et al., 2015, 2019; Sillett & Van Pelt, 2000, 2007). Although these studies have contributed to many aspects of redwood ecology including crown complexity and physiology, conducting large-scale surveys using these methods would be extremely time intensive and costly. Fortunately, in recent decades, remote sensing has proven to be a powerful tool for conducting forest monitoring at multiple scales (Maxwell et al., 2017; Wulder et al., 2006). In particular, classification of aerial imagery

has documented the spatial extent of tree health following disturbance events (Gartner et al., 2015; Hart et al., 2015; Kantola et al., 2010; Maxwell et al., 2017; Näsi et al., 2015), including redwood mortality following fires (Bishop et al., 2014).

The increasing accessibility of high-resolution imagery provides an opportunity to conduct large scale forest health assessments in an accurate and cost-effective manner. For example, the National Agriculture Imagery Program (NAIP) produces publicly available high-resolution (<1 m) aerial imagery across the contiguous United States, and the inclusion of a near-infrared band in recent data acquisitions has increased its potential to perform vegetation health assessments at refined scales. Furthermore, the integration of aerial imagery with other remotely sensed data such as Light Detection and Ranging (LiDAR) data has been utilized to increases the accuracy of forest condition assessments (Bishop et al., 2014; Maxwell et al., 2017) as well as provide valuable information about forest structure (Kane et al., 2010, 2014; North et al., 2017). Concurrent analysis of hyperspectral aerial imagery and LiDAR data has also been applied to map secondary forests of redwoods to provide valuable species distribution maps with high levels of accuracy (Francis et al., 2020; Francis & Asner, 2019). Here, we use publicly available remote sensing data, NAIP imagery and discrete-return LiDAR, to map the spatial distribution of crown health in the old-growth redwood forest of Humboldt Redwood State Park (HRSP).

The overall objective of this study was to investigate the spatial patterns and drivers of crown dieback in HRSP. To do so we integrated Random Forests (RF) classifications (Breiman, 2001) of NAIP imagery with individual tree extents derived from LiDAR to create a detailed map of healthy trees and trees with crown dieback. To

better understand potential drivers of crown deterioration, we also used RF to explore the relationship between crown health and environmental variables such as terrain and proximity to different forest edges, including streams, roads, and other vegetation cover types as well as tree height. We hypothesized that crown dieback would be H1): more prevalent near anthropogenic edges such as roads that expose trees to the adverse conditions of a forest edge and alter local hydrology, and H2): elevated in areas where multiple edge types intersect or are in close proximity, potentially amplifying the impacts of edge effects on redwood forests.

Methods

Site Description

Our study was conducted within the Eel River watershed, and was constrained to alluvial flats and adjacent lower slopes that contain the greatest densities of tall old-growth redwoods forests within HRSP (Figure 3-1). HRSP is located in northwestern California (40.31°N, 123.98°W) and has a Mediterranean climate with wet winters and dry summers with fog inundation at lower elevations in the late summer months. The area receives an average annual rainfall of 1,300 mm, and summer temperatures range from 10-24°C and winter temperatures range from 4-12°C. The park is 53,000 ha and contains the largest remaining contiguous tract of old-growth forest, hosting approximately 80% of all known trees >107 m tall (Van Pelt et al., 2016). HRSP is relatively narrow and runs along the Bull Creek and lower South Fork Eel River. Like most other redwood parks and preserves, many areas surrounding and within HRSP underwent clear-cutting at least once and often twice in the past 150 years, which has created abrupt, artificial edges

along a large proportion of the remaining old-growth forest. Presently, residential and commercial properties and agricultural fields frequently border the park in addition to Highway 101 and other tourist byways (e.g., Avenue of the Giants).

Remote Sensing Data

In this study, we followed multiple steps to integrate spectral information from NAIP imagery with the structural information of LiDAR, which resulted in a bivariate point pattern of crown health (Figure 3-2). NAIP imagery for 2016 and 2018 (Figure 3-3A) was obtained from the United States Geologic Survey (USGS) EarthExplorer (https://earthexplorer.usgs.gov/). Each image consisted of four spectral bands (R, G, B, NIR) in an 8-bit radiometric resolution characterized by a 0.6 m spatial resolution. For both years of NAIP imagery, tiles were mosaicked into a single raster that covered the full extent of HRSP's boundaries. The inclusion of a NIR band in recent data acquisitions allows calculation of a Normalized Difference Vegetation Index (NDVI; Tucker 1979). A vegetation index, like NDVI, is particularly well suited to detect crown dieback compared to individual spectral bands or natural color (Bannari et al., 1995). For each year we calculated NDVI using the R and NIR bands:

$$NDVI = \frac{NIR-R}{NIR+R} \qquad \text{Equation 1}$$

We also conducted principal components analysis (PCA) on the original four bands to serve as additional predictor variables for the RF classifications. The original NAIP imagery bands (R, G, B, NIR), an NDVI layer, and the PCA layers were then used for training and prediction in each RF classification. We used NAIP datasets from two

different years to minimize artifacts associated with varying viewing angles, illumination, and shadows in each NAIP dataset (Maxwell et al., 2017).

Discrete-return LiDAR data were obtained from the USGS National Map (https://viewer.nationalmap.gov/basic/) for the full extent of the park (USGS, 2020). The LiDAR data were acquired from 2018-2019 and made publicly available in 2020 with an average point density of 6.7 points/m². LiDAR data were downloaded as individual tiles with a 1000 m X 1000 m footprint in the American Society for Photogrammetry and Remote Sensing (ASPRS) LAS format and points were classified into two categories, ground or non-ground. Each tile was reprojected to fit the projection of the NAIP imagery, Universal Transverse Mercator (UTM) Zone 10N, using the LAStools 'las2lasPro (project)' tool (Isenburg, 2019) prior to any further processing or analysis.

Canopy Height Modeling and Tree Detection

To identify individual tree crowns, we performed individual tree detection (ITD) on a LiDAR-derived canopy height model (CHM). Raw LiDAR data are obtained as a 3-D point cloud of elevation values, so prior to canopy height modeling and ITD, the LiDAR data was normalized to extract the relative height of each point. During normalization, a digital terrain model (DTM) was subtracted from all non-ground classified points to convert the elevation value of each point to obtain its height above the ground. The DTM was computed on-the-fly in which ground classified points were interpolated using Delaunay triangulation. Using the height normalized point cloud, a CHM with a 1 m resolution was generated using the "pit-free" algorithm proposed by Khosravipour et al. (2014) (Figure 3-3B). Pixels that contained spurious height values such as values below 0 m or heights above 115 m were eliminated from the CHM prior to

ITD. The maximum height value was selected by inspecting pixels near the upper limit of redwood height, ~115 m (Sillett et al., 2015) and also by determining that the tallest tree in HRSP was ~113 m. We also confirmed that the pixels above 113 m belonged to sensor errors or atmospheric interference. ITD was performed on the CHM using a watershed algorithm (Pau et al., 2010) and a minimum height threshold of 60 m was used to obtain only canopy dominant or codominant trees (Figure 3-3C). All LiDAR data normalization, canopy height modeling, and ITD was conducted using the *lidR* package (Roussel & Auty, 2020) in R (R Core Team, 2018).

Crown Health Classifications

Random forest models (Breiman, 2001) were implemented in the *randomForest* R package (Liaw & Wiener, 2002) to classify pixels of NAIP imagery into three classes: crown dieback, healthy crown, or shadow. We selected random forest as the classification method because it can efficiently capture non-linear and complex interactions between predictors variables and has been shown to as accurate if not more so than other parametric methods (Cutler et al., 2007). A random forest is a nonparametric ensemble model that aggregates a set of decision trees to perform classifications and regression. Each tree is built using bootstrapped training data and a recursive partitioning approach that divides data into subgroups or nodes based on the homogeneity of the response variable. For each split, a random subset of predictor variables is considered as candidates to divide the node and the RF algorithm selects the predictor variable that maximizes node homogeneity. Individual trees are built until group homogeneity can no longer be increased. Following the construction of the forest, new data is passed through each tree in the ensemble and predictions are made by majority vote (classification) or

averaging (regression) the predictions from all of the trees in the ensemble. Because RFs are constructed using bootstrapping, the samples withheld during model fitting or out-of-bag (OOB) samples can be used as cross-validation to measure a model's overall accuracy or OOB error. Lastly, RF models can also produce measurements of variable importance. To determine the relative importance of each predictor variable, the values of each single predictor variable is randomly permutated in the OOB samples and those now modified OOB samples are used to make a prediction in the RF model. The importance of the permutated variable is then calculated as the difference in model accuracy, as determined by either the increase of mean square error (%MSE) or the mean decrease in accuracy (MDA), between the out-of-bag error and the new modified OOB error. The permutation of each predictor variable breaks any associations it has with the response variable and any interactions it may have with other predictor variables. Therefore, the variable importance metric reflects the influence that each predictor has on the response variable including any multivariate interactions with other predictor variables without explicitly modelling them (Breiman, 2001; Cutler et al., 2007).

Random forest models were trained using unique training points that were produced by visually inspecting each image and manually assigning points for each class: crown dieback, healthy crown, or shadow. Initially 200 training points were generated for each class, however after the initial classifications of each dataset, it was apparent that additional training points were needed to capture more variation in the healthy crown class primarily due to variation in brightness. For example, healthy crowns that were generally brighter in the 2016 NAIP imagery were often misclassified as crown dieback and more training points were needed to capture the variation in brightness of the healthy

crowns. Consequently, 25 more points were added to each dataset's healthy crown training points. Following these additions, training data for each set of imagery consisted of 625 points (200 crown dieback, 225 healthy crowns, and 200 shadow) which were then used to train random forest classification models. Nine bands of imagery, including the original four bands of NAIP imagery and five derived layers (NDVI and PCs 1-4) were used as predictor variables. We used 500 trees to build each RF model and three predictor variables were considered at each split. Following classification, a pixel size filter was applied to each classification to remove any areas of dieback that contained less than <2 pixels which may have been misclassified.

Because NAIP data is a type of aerial imagery, areas can have different viewing angles depending on their distance from the flight path. Areas that were farther from the flight path were off-nadir and were more likely to alter the spatial accuracy of the classification and introduce false positives of crown dieback because trees in these areas falsely appeared tilted over other features such as roads, rivers, and bare ground in the imagery. All of these non-canopy features have similar spectral values to crown dieback, and due to the low spectral resolution of the NAIP imagery, they could not be classified separately. To reduce false positives, we visually inspected each old-growth area and removed any non-canopy pixels that were misclassified as crown dieback. Following the removal of erroneous pixels, we georectified the classifications to correct for geospatial inaccuracies that would have been caused by tilting. Georectification was conducted by visually comparing the crowns in the imagery with the pattern of individual tree crowns that we identified using the CHM. The "Adjust" transformation in ArcMap was used for all adjustments. Many flight paths were used during the imagery acquisition of the park,

so we conducted the georectification in segments and then recreated a mosaic for crown intersections.

Old Growth Boundaries and Edge Features

In HRSP, redwoods dominate low-lying landscape positions, however because the park is both farther inland and drier than the other northern National and State Parks, the high density of redwoods quickly transitions to mixed conifer forest at slightly higher elevations (Busing & Fujimori, 2002; Sawyer et al., 2000; Van Pelt et al., 2016). We restricted our analyses to the low-lying areas of HRSP because the dominance of redwoods in these areas allows for accurate identification of redwoods with healthy or dieback crowns while the nearly continuous dense canopy limits the amount of exposed ground. This is particularly important when using NAIP imagery as its spectral resolution is fairly coarse and ground features have similar spectral values to crown dieback. We identified lowland old-growth areas using previous vegetation surveys conducted by the California State Parks Department and adjusted the boundaries based on stand height and density using the CHM.

We delineated features that adjoin edges of the old-growth areas including roads, rivers, and other vegetation in order to differentiate between different types of edge effects. Road and river boundaries were edited from the U.S. Census Bureau's Topologically Integrated Geographic Encoding and Referencing (TIGER) Database and National Hydrography Dataset (NHD). These features were obtained as line geometries, but were converted to polygons via digitizing using GPS points, LiDAR, and both NAIP imagery datasets to accurately represent the spatial extent of their boundaries. Roads were further categorized as either Highway 101 or other smaller, secondary roads which

included the Avenue of the Giants and other two-lane roadways. Smaller private roads that could not be accurately mapped were excluded from our analyses. Other vegetation areas that included non-old growth forest such as agricultural fields, secondary forest, and residential areas were also delineated using LiDAR, NAIP imagery, and the California Parks Department surveys. Along the highway there are often areas of non-old growth vegetation that separated old-growth stands from the road. We considered these areas as separate forest edges if they extended farther than 30 m from the road and included them as other vegetation. For each tree extracted during ITD, we calculated the distance to the nearest edge type (i.e., roads, rivers, and other vegetation). We also included a metric of topographic heterogeneity, the terrain ruggedness index (TRI), to capture the impact that the changes in local topography may have had crown health (Madej, 2010). Cut-and-fill construction methods and increased erosion rates caused by previous road installations and logging activities and typical can alter local topography and hydrology (Madej, 2010). For redwoods neighboring these areas, these activities can result in the partial denudation of roots which in turn can affect crown health. TRI measures the absolute difference in elevation of a central cell and its surrounding areas (Riley et al., 1999). We calculated TRI at a 5 m resolution with a 11×11 window, which approximates a 30 m radius from center cell. This window size was selected in order to capture the topographic heterogeneity surrounding a central redwood tree, with knowledge that the rooting extent of old redwoods can have been noted to reach 30 m (California State Parks, n.d.)

Crown Intersections and Validation

We intersected the RF classifications and individual tree extents using only dieback classified pixels. The presence or absence of dieback pixels in a delineated crown extent was then used to designate each tree as dieback or healthy. We then extracted the centroid of each tree extent to create a bivariate point pattern of crown health. To assess the accuracy of the workflow outlined in Figure 3-2, we collected field validation data using a sub-meter GPS device (Juniper Geode, https://www.junipersys.com/) following a visual crown health assessment. We collected GPS points for 59 trees with crown dieback and 54 trees with healthy crowns. Multiple GPS points were collected radially around each tree and were later averaged to determine the center location of each tree. We performed the accuracy assessment by contrasting the crown health status of each tree that we identified in the field with the crown health status of that same tree that was produced in the workflow (Jensen, 2015).

Spatial Patterns of Crown Dieback

Kernel density estimation (KDE) was used to visualize the spatial patterns of crown health at the scale of the park. Overall tree density and the density of healthy and dieback trees was calculated at a 5 m resolution using an isotropic Gaussian kernel and 30 m smoothing bandwidth. The resolution and smoothing bandwidth parameters were selected to produce high-resolution (5 m) map of redwoods that captured local density (30 m) of individual redwoods while also minimizing the computational demands of higher resolved maps (5 m vs. 1 m). The probability of crown dieback was then determined by calculating the ratio of dieback density relative to overall tree density. Given that the boundaries of our study area signify transitions from redwood-dominated

stands to either non-forested areas or mixed conifer forest, we did not include any edge corrections in our density or probability estimates (Baddeley et al., 2015). All density and probability estimations were conducted using the *spatstat* R package (Baddeley et al., 2015; Baddeley & Turner, 2005).

Following density and probability mapping, there was a clear dichotomy between the northern portion of the park which contained large aggregations of crown dieback and all other areas of the park where crown dieback was more sporadic (Figure B-2). We therefore conducted separate analyses for the "northern" and "southern" portions of HRSP (Figure 3-1) when examining the potential influence of environmental variables such as distance to edge features and topography, as well as tree height and density. For each region, we examined the relative importance of explanatory variables using RF regression. To determine whether the distributions of each variable for healthy and dieback trees were significantly different ($p < 0.05$), we used the two-sample Kolmogorov-Smirnov test.

Results

Aerial Imagery and LiDAR Integration

Individual tree detection identified 31,901 trees in the low-lying old-growth areas of HRSP (Figure 3-3). A total of 1,288 (4.0%) of those trees were classified as having crown dieback, while 30,613 trees (96.0%) had healthy crowns. Both RF classifications for each year of imagery had low OOB error; the NAIP 2016 classification had an overall accuracy of 99.8% (Table 3-1) while the classification of NAIP 2018 imagery achieved 100% overall accuracy (Table 3-2). Relative importance of each classification indicated

that NDVI and the first PC were the most important variables for discerning spectral variation in the three classes (crown dieback, healthy crown, and shadow). For the NAIP 2016 classification, NDVI was the most important variable followed by the first PC, whereas, for the NAIP 2018 classification, the ranking order was reversed (Figure B-1). The accuracy assessment using field validation data showed that the workflow outlined in Figure 3-2 correctly identified the crown health status of individual redwoods with 93.4% accuracy. Of the 113 trees measured during field validation, all 54 trees with healthy crowns were correctly identified using the workflow and 52 of the 59 dieback trees were also correctly identified.

Spatial Patterns of Crown Dieback

Overall, the prevalence of crown dieback in old redwoods was relatively low across most of the park. However, the prevalence of crown dieback varied regionally and substantially higher rates of dieback were observed in the northern portion of the park (Figure 3-5). This area contained approximately 56% of all dieback trees while containing only 17% of the total study area. In the northern portion of the park, the probability of dieback was especially high near Highway 101 and other secondary roads, particularly where they come in close proximity to each other as well as other clearcut forests or riparian areas (Figure 3-5). The aggregation of crown dieback also coincided in areas where overall tree density was low (Figure 3-7G & Figure B-3).

The distributions of environmental variables for trees in the southern portions of the park showed that healthy and dieback trees generally had similar environmental variables and local tree density, but the distributions of height and proximity to roads were significantly different ($p<0.05$; Figure 3-6A-G). For the northern portion of the

park, the distribution of environmental variables showed that dieback trees had higher proportions of their population near forest edges including Highway 101, secondary roads, other vegetation, and streams relative to healthy trees (Figure 3-7A-D). The distributions of tree height and local density between healthy and dieback trees were also significantly different ($p<0.05$), with dieback trees tended to be taller trees and have lower neighborhood density. The distributions of TRI values were significantly different between healthy and dieback trees in this area, with dieback trees typically located in more rugged terrain ($p<0.05$; Figure 3-7E). The RF model for the north portion of the park described ~25% of the variation in crown health in the area. Within this RF model, variable importance analyses indicated that tree height was the most important variable when discerning crown health status followed by the three types of anthropogenic edges (Highway 101, other vegetation, and secondary roads), tree density, edges associated with stream channels, and local topographic variation as indicated by TRI. Results from a RF model fitted to the other area of the park are not reported here because model performance was extremely low (near 0% variance explained).

Discussion

Aerial Imagery and LiDAR Integration

We identified the crown health status of more than 30,000 canopy trees in old growth coast redwood forests of Humboldt Redwoods State Park (HRSP). While our accuracy assessment showed that we captured crown deterioration with a high degree of accuracy, we also acknowledge the limitations of aerial imagery and LiDAR data especially in the context of a redwood ecosystem. Individual tree detection (ITD) can be

useful for estimating forest inventory metrics such as height and crown radius, however it also frequently underestimates smaller trees (Jeronimo et al., 2018). While we did not explicity test for the commission and omission error in our ITD methods, we did observe cases where the canopies of shorter trees were merged into the delineated tree extents of taller adjacent trees (Figure 3-3C). We suspect that the underestimation of smaller trees can largely be attributed to redwoods' ability to regenerate via basal sprouting (Fritz, 1932; Sillett & Van Pelt, 2000, 2007). Prolific regeneration in a relatively small area can result in dense canopies with a strong degree of crown overlap and therefore limited crown differentation between canopy dominant trees and the smaller reiterated trunks. Similar inclusion of multiple crowns into a "single" tree extent was also found in other studies that have utilitized LiDAR to derive height and density metrics in redwood forests (Van Pelt et al., 2016). Although smaller trees tend to be underestimated during ITD, we believe this did not signficantly impact our results as we were focused on the crown deterioration of tall trees (>60m) which have been shown to be detected at higher accuracies (Jeronimo et al., 2018).

Similar to ITD, issues of varying view angles, illumination, and a lack of crown differentiation have also reduced tree identification and classfication accuracy in previous studies that have used aerial imagery particularly in smaller trees (Baguskas et al., 2014; Maxwell et al., 2017). However, we performed classifications on NAIP images from two different years to minimize the occurrence of false negatives that would have occurred due to shadowing or poor viewing angle in a single dataset (Maxwell et al., 2017). We also verified all trees that were misclassified in our accuracy assessment were not shaded in both image years, and mean height of the misclassifed trees was the same or higher

than the overall tree mean height and mean height of trees with dieback, indicating that neither variation in lighting nor tree height substantially impacted the accuracy of the results. We suspect that the underrespresentation of dieback trees in our accuracy assessment may be partially attributed to redwoods with “spiked-tops” or crown dieback in which the lateral branches have broken off, leaving just the main trunk (Fritz, 1932). The excision of the dead lateral branches reduces the total surface area of crown that could be detected as dieback during classification. In turn, the number of dieback trees detected in this study is likely underestimated. Despite the challenges of using NAIP imagery and ITD methods, this study supports previous findings that the integration of aerial imagery and LiDAR can provide a valuable and cost effective methodology for conducting forest health assessments (Baguskas et al., 2014; Bishop et al., 2014; Maxwell et al., 2017). Furthermore, NAIP imagery is free, covers the entire extent of the redwood distribution, and is acquired semi-frequently depending on government funding. Hence, the methodology described and demonstrated here can be repeated to conduct ongoing health assessments at HRSP and also can be employed to assess the canopy health of other redwood forest reserves and perhaps other forest types as well.

Implications for the Redwood Ecosystem

Across all areas of the park, height appeared to be the most important and consistent variable related to crown health. The apparent heightened susceptibility to crown dieback for taller trees is likely due to the effects the increasing hydrostatic gradient in water potential that challenges physiological function in extremely tall tree species (Domec et al., 2010; Koch et al., 2004). Moreover, taller trees tend to have a larger proportions of their crown exposed to intense sunlight and wind and be more

susceptible to windthrow (Laurance & Curran, 2008; Van Pelt et al., 2016). However, where crown dieback was aggregated in the northwest portion of HRSP, trees had lower average tree heights (80 m) compared to other areas where crown dieback was less prevalent (82 m) suggesting that the hydraulic constraints that height places on water transport is not the sole driver of crown deterioration.

The aggregation of crown deterioration near edges in the northwestern portion of HRSP and its relationship with distance to specific edge features suggest that anthropogenic disturbances have led to higher rates of crown dieback, but that these effects have primarily impacted taller trees in those locations (Figure 3-7 & Figure 3-8). These findings are consistent with previous studies that found artificial forest edges and particularly roads create adverse microclimates that induced drought stress and that taller trees are impacted more severely by these effects (Goosem, 2007; Harper et al., 2005; Laurance et al., 2009; Laurance & Curran, 2008; Russell et al., 2000). Crown dieback also coincided with lower overall tree density in the northern portion of the park (Figure B-3). These lower densities of trees may indicate increases in recent windthrow events which is the leading cause of mortality for large redwoods (Van Pelt et al. 2016) and leading to higher exposure along these edges (Laurance & Curran, 2008). However, this would require further research and mapping of snags and down logs to determine if windthrow caused tree density to be lower in these areas. Although proximity to streams was not the most important variable in our RF analysis (Figure 3-8), we did observe notable increases in dieback rates in several meanders along sections of certain streams (e.g. Figure 3-4). This is likely indicative of previous flood events in which sustained

water inundation of the roots has resulted in concentrated occurrences of dieback and mortality (Lorimer et al., 2009; Stone & Vasey, 1968).

While our results show large variations in distances over which edge disturbances have impacted redwoods, the aggregation of dieback in northern portion of HRSP indicates that trees in this area were particularly sensitive to the habitat fragmentation that was driven by the near ubiquitous clear-cut logging, road building and other expansion of human influence on the landscape over the past two centuries. The creation of abrupt, artificial forest boundaries following land cover changes has increased sunlight and wind exposure for the remaining trees near the forest edge, and the installations of permanent roads and highways has had further implications by altering hydrology (Bocking et al., 2017; Jones, 2000; Laurance et al., 2009), increasing drought stress (Chapter 1), and has acted as the inciting factor for previous landslides (Madej, 2010). While these edge effects could have been minimized by allowing previously harvested forest to grow back and thereby buffering the remaining trees from desiccation, most areas that were logged in the 19th and 20th centuries were harvested multiple times, so the proportion of mature secondary forest in the redwood distribution is even less than remaining old-growth area (Burns et al., 2018).

The rates of crown dieback were generally low across our study area, however the aggregation of dieback in the northwestern portion of the park and in taller trees warrants concern. For this study we only analyzed the spatial distribution of crown dieback, which is presumably associated with hydraulic failure and embolism in the xylem during a discrete drought stress event (sensu Tyree & Sperry, 1988). These events cause redwood trees to be characterized by large primary branches and tree tops that are dead and which

are visible for years to decades. Although the canopies of these trees often recover through epicormic sprouting, it is uncertain whether this mechanism of recovery is sufficient to avoid an increased likelihood of mortality over the long term. We suspect that although redwoods are highly rot-resistant, that dieback will provide entryways for wood decaying fungi that may increase the likelihood of further injury and windthrow over the course of decades to centuries. In recent decades, drought-induced mortality has become more widespread across multiple species (Allen et al., 2010) and larger trees have been shown to be impacted by drought-induced mortality more severely across a wide range of forest types (Bennett et al., 2015). These trends in drought stress and mortality in large trees are particularly concerning considering that large trees disproportionally influence many aspects of forest structure and function including biomass, structure, and habitat suitability for many species (Burns et al., 2018; Lutz et al., 2012, 2013; Sillett et al., 2010, 2015; Van Pelt et al., 2016) including the endangered marbled murrelet and northern spotted owl in the redwood distribution (Burns et al., 2018). The climatic influences of the coast have previously buffered redwoods from some of the most severe droughts of the past 1,000 years (Voelker et al., 2018). However, declines in fog frequency during the past century and climate projections suggest that the climatic stability of the redwood distribution may be dwindling which could substantially influence the future extent of the redwood distribution (Fernández et al., 2015; Johnstone & Dawson, 2010). HRSP is near the furthest extent inland to which marine layer fog can currently reach. If warming trends in the ocean and atmosphere continue to dissipate the frequency or intensity of these fog events, tall old redwood trees

at HRSP and other similar locations may be particularly vulnerable to increased drought stress combined that could be exacerbated by forest edge conditions.

Conclusion

By quantifying the prevalence of crown dieback within HRSP, we were able to delineate areas of old-growth redwood forest that have been significantly impacted by previous landcover changes and may be in need of increased conservation efforts. As climate change and habitat fragmentation continue to threaten redwood extent, further study is needed to determine how to best mitigate the potential for large-scale redwood range contractions in the future. Toward this end, roads and other forest edges should be considered as having a strong influence on the health of large redwood trees. We also show that publicly available remote sensing data, NAIP imagery and LiDAR, can be coupled with random forest classifications and ITD methods to conduct large scale spatial health assessments of redwoods at the individual tree level. These data sources have the potential to be used for repeated health assessments across the redwood distribution in the future.

References

Allen, C. D., Macalady, A. K., Chenchouni, H., Bachelet, D., McDowell, N., Vennetier, M., Kitzberger, T., Rigling, A., Breshears, D. D., Hogg, E. H. (Ted), Gonzalez, P., Fensham, R., Zhang, Z., Castro, J., Demidova, N., Lim, J. H., Allard, G., Running, S. W., Semerci, A., & Cobb, N. (2010). A global overview of drought and heat-induced tree mortality reveals emerging climate change risks for forests. *Forest Ecology and Management*, *259*(4), 660–684.

https://doi.org/10.1016/j.foreco.2009.09.001

Ambrose, A. R., Baxter, W. L., Wong, C. S., Næsborg, R. R., Williams, C. B., & Dawson, T. E. (2015). Contrasting drought-response strategies in California redwoods. *Tree Physiology*, *35*(5), 453–469. https://doi.org/10.1093/treephys/tpv016

Ambrose, A. R., Sillett, S. C., & Dawson, T. E. (2009). Effects of tree height on branch hydraulics, leaf structure and gas exchange in California redwoods. *Plant, Cell and Environment*, *32*(7), 743–757. https://doi.org/10.1111/j.1365-3040.2009.01950.x

Baddeley, A., Rubak, E., & Turner, R. (2015). *Spatial Point Patterns: Methodology and Applications with {R}*. Chapman and Hall/CRC Press. http://www.crcpress.com/Spatial-Point-Patterns-Methodology-and-Applications-with-R/Baddeley-Rubak-Turner/9781482210200/

Baddeley, A., & Turner, R. (2005). {spatstat}: An {R} Package for Analyzing Spatial Point Patterns. *Journal of Statistical Software*, *12*(6), 1–42. http://www.jstatsoft.org/v12/i06/

Baguskas, S. A., Peterson, S. H., Bookhagen, B., & Still, C. J. (2014). Evaluating spatial patterns of drought-induced tree mortality in a coastal California pine forest. *Forest Ecology and Management*, *315*, 43–53. https://doi.org/10.1016/j.foreco.2013.12.020

Bannari, A., Morin, D., Bonn, F., & Huete, A. R. (1995). A review of vegetation indices. *Remote Sensing Reviews*, *13:1-2*, 95–120. https://doi.org/10.1080/02757259509532298

Bennett, A. C., McDowell, N. G., Allen, C. D., & Anderson-Teixeira, K. J. (2015). Larger trees suffer most during drought in forests worldwide. *Nature Plants*, *1*, 15139. https://doi.org/10.1038/nplants.2015.139

Bishop, B., Dietterick, B., White, R., & Mastin, T. (2014). Classification of Plot-Level Fire-Caused Tree Mortality in a Redwood Forest Using Digital Orthophotography and LiDAR. *Remote Sensing*, *6*(3), 1954–1972. https://doi.org/10.3390/rs6031954

Bocking, E., Cooper, D. J., & Price, J. (2017). Using tree ring analysis to determine impacts of a road on a boreal peatland. *Forest Ecology and Management*, *404*, 24–30. https://doi.org/10.1016/j.foreco.2017.08.007

Breiman, L. (2001). Random Forests. *Machine Learning*, *45*, 5–32. https://doi.org/10.1023/A:1010933404324

Burgess, S., & Dawson, T. E. (2004). The contribution of fog to the water relations of Sequoia sempervirens (D. Don): Foliar uptake and prevention of dehydration. *Plant, Cell and Environment*, *27*, 1023–1034. https://doi.org/10.1111/j.1365-3040.2004.01207.x

Burns, E. E., Campbell, R., & Cowan, P. D. (2018). *State of Redwoods Conservation Report: A Tale of Two Forests*. https://www.savetheredwoods.org/wp-content/uploads/State-of-Redwoods-Conservation-Report-Final-web.pdf

Busing, R. T., & Fujimori, T. (2002). Dynamics of composition and structure in an old Sequoia sempervirens forest. *Journal of Vegetation Science*, *13*(6), 785–792. https://doi.org/10.1111/j.1654-1103.2002.tb02108.x

California State Parks. (n.d.). *About Coast Redwoods*. https://www.parks.ca.gov/?page_id=22257

Carroll, A. L., Sillett, S. C., & Kramer, R. D. (2014). Millennium-scale crossdating and inter-annual climate sensitivities of standing California redwoods. *PLoS ONE*, *9*(7). https://doi.org/10.1371/journal.pone.0102545

Carroll, A. L., Sillett, S. C., & Van Pelt, R. (2018). Tree-Ring Indicators of Fire in Two Old-Growth Coast Redwood Forests. *Fire Ecology*, *14*(1), 85–105. https://doi.org/10.4996/fireecology.140185105

Cutler, D. R., Edwards, T. C., Beard, K. H., Cutler, A., Kyle, T., Gibson, J., Lawler, J. J., Beard, H., & Hess, T. (2007). Random Forests for Classification in Ecology. *Ecology*, *88*(11), 2783–2792.

Dawson, T. E. (1998). Fog in the California redwood forest: ecosystem inputs and use by plants. *Oecologia*, *117*, 476–485.

Domec, J. C., Schäfer, K., Oren, R., Kim, H. S., & McCarthy, H. R. (2010). Variable conductivity and embolism in roots and branches of four contrasting tree species and their impacts on whole-plant hydraulic performance under future atmospheric CO2 concentration. *Tree Physiology*, *30*(8), 1001–1015. https://doi.org/10.1093/treephys/tpq054

Fernández, M., Hamilton, H. H., & Kueppers, L. M. (2015). Back to the future: using historical climate variation to project near-term shifts in habitat suitable for coast redwood. *Global Change Biology*, *21*(11), 4141–4152. https://doi.org/10.1111/gcb.13027

Francis, E. J., & Asner, G. P. (2019). High-resolution mapping of redwood (*Sequoia sempervirens*) distributions in three Californian forests. *Remote Sensing*, *11*(3), 1–19. https://doi.org/10.3390/rs11030351

Francis, E. J., Asner, G. P., Mach, K. J., & Field, C. B. (2020). Landscape scale variation in the hydrologic niche of California coast redwood. *Ecography*, *43*, 1–11. https://doi.org/10.1111/ecog.05080

Fritz, E. (1929). Some popular fallacies concerning California redwood. *Madroño 1*, 221–224.

Fritz, E. (1932). The role of fire in the redwood region. *University of California Agricultural Experiment Station Circular*, 323.

Gartner, M. H., Veblen, T. T., Leyk, S., & Wessman, C. A. (2015). Detection of mountain pine beetle-killed ponderosa pine in a heterogeneous landscape using high-resolution aerial imagery. *International Journal of Remote Sensing*, *36*(21), 5353–5372. https://doi.org/10.1080/01431161.2015.1095369

Goosem, M. (2007). Fragmentation impacts caused by roads through rainforests. *Current Science*, *93*(11), 1587–1595.

Harper, K. A., Macdonald, S. E., Burton, P. J., Chen, J., Brosofske, K. D., Saunders, S. C., Euskirchen, E. S., Roberts, D., Jaiteh, M. S., & Esseen, P.-A. (2005). Edge Influence on Forest Structure and Composition in Fragmented Landscapes. *Conservation Biology*, *19*(3), 768–782. https://doi.org/10.1111/j.1523-1739.2005.00045.x

Hart, S. J., Schoennagel, T., Veblen, T. T., Chapman, T. B., & Franklin, J. (2015). Area burned in the western United States is unaffected by recent mountain pine beetle outbreaks. *Proceedings of the National Academy of Sciences of the United States of America*, *112*(14), 4375–4380. https://doi.org/10.1073/pnas.1424037112

Isenburg, M. (2019). *LAStools - efficient LiDAR processing software* (No. 200131,

unlicensed). http://rapidlasso.com/LAStools

Jensen, J. R. (2015). *Introductory Digital Image Processing: A Remote Sensing Perspective* (4th ed.). Prentice Hall Press.

Jeronimo, S. M. A., Kane, V. R., Churchill, D. J., McGaughey, R. J., & Franklin, J. F. (2018). Applying LiDAR individual tree detection to management of structurally diverse forest landscapes. *Journal of Forestry*, *116*(4), 336–346. https://doi.org/10.1093/jofore/fvy023

Johnstone, J. A., & Dawson, T. E. (2010). Climatic context and ecological implications of summer fog decline in the coast redwood region. *Proceedings of the National Academy of Sciences of the United States of America*, *107*(10), 4533–4538. https://doi.org/10.1073/pnas.0915062107

Johnstone, J. A., Roden, J. S., & Dawson, T. E. (2013). Oxygen and carbon stable isotopes in coast redwood tree rings respond to spring and summer climate signals. *Journal of Geophysical Research: Biogeosciences*, *118*(4), 1438–1450. https://doi.org/10.1002/jgrg.20111

Jones, J. A. (2000). Hydrologic processes and peak discharge response to forest removal, regrowth, and roads in 10 small experimental basins, Western Cascades, Oregon. *Water Resources Research*, *36*(9), 2621–2642. https://doi.org/10.1029/2000WR900105

Kane, V. R., McGaughey, R. J., Bakker, J. D., Gersonde, R. F., Lutz, J. A., & Franklin, J. F. (2010). Comparisons between field- and LiDAR-based measures of stand structural complexity. *Canadian Journal of Forest Research*, *40*(4), 761–773. https://doi.org/10.1139/X10-024

Kane, V. R., North, M. P., Lutz, J. A., Churchill, D. J., Roberts, S. L., Smith, D. F., McGaughey, R. J., Kane, J. T., & Brooks, M. L. (2014). Assessing fire effects on forest spatial structure using a fusion of Landsat and airborne LiDAR data in Yosemite National Park. *Remote Sensing of Environment*, *151*, 89–101. https://doi.org/10.1016/j.rse.2013.07.041

Kantola, T., Vastaranta, M., Yu, X., Lyytikainen-Saarenmaa, P., Holopainen, M., Talvitie, M., Kaasalainen, S., Solberg, S., & Hyyppa, J. (2010). Classification of Defoliated Trees Using Tree-Level Airborne Laser Scanning Data Combined with Aerial Images. *Remote Sensing*, *2*, 2665–2679. https://doi.org/10.3390/rs2122665

Khosravipour, A., Skidmore, A. K., Isenburg, M., Wang, T., & Hussin, Y. A. (2014). Generating pit-free canopy height models from airborne lidar. *Photogrammetric Engineering and Remote Sensing*, *80*(9), 863–872. https://doi.org/10.14358/PERS.80.9.863

Koch, G. W., Stillet, S. C., Jennings, G. M., & Davis, S. D. (2004). The limits to tree height. *Nature*, *428*(6985), 851–854. https://doi.org/10.1038/nature02417

Laurance, W. F., & Curran, T. J. (2008). Impacts of wind disturbance on fragmented tropical forests: A review and synthesis. *Austral Ecology*, *33*, 399–408. https://doi.org/10.1111/j.1442-9993.2008.01895.x

Laurance, W. F., Goosem, M., & Laurance, S. G. W. (2009). Impacts of roads and linear clearings on tropical forests. *Trends in Ecology and Evolution*, *24*(12), 659–669. https://doi.org/10.1016/j.tree.2009.06.009

Laurance, W. F., Nascimento, H. E. M., Laurance, S. G., Andrade, A., Ewers, R. M.,

Harms, K. E., Luizão, R. C. C., & Ribeiro, J. E. (2007). Habitat fragmentation, variable edge effects, and the landscape-divergence hypothesis. *PLoS ONE*, *2*(10). https://doi.org/10.1371/journal.pone.0001017

Liaw, A., & Wiener, M. (2002). Classification and Regression by randomForest. *R News*, *2*(3), 18–22. https://cran.r-project.org/doc/Rnews/

Lorimer, C. G., Porter, D. J., Madej, M. A., Stuart, J. D., Veirs, S. D., Norman, S. P., O'Hara, K. L., & Libby, W. J. (2009). Presettlement and modern disturbance regimes in coast redwood forests: Implications for the conservation of old-growth stands. *Forest Ecology and Management*, *258*(7), 1038–1054. https://doi.org/10.1016/j.foreco.2009.07.008

Lutz, J. A., Larson, A. J., Freund, J. A., Swanson, M. E., & Bible, K. J. (2013). The Importance of Large-Diameter Trees to Forest Structural Heterogeneity. *PLOS ONE*, *8*(12), 1–13. https://doi.org/10.1371/journal.pone.0082784

Lutz, J. A., Larson, A. J., Swanson, M. E., & Freund, J. A. (2012). Ecological Importance of Large-Diameter Trees in a Temperate Mixed-Conifer Forest. *PLOS ONE*, *7*(5), 1–15. https://doi.org/10.1371/journal.pone.0036131

Madej, M. A. (2010). Redwoods, restoration, and implications for carbon budgets. *Geomorphology*, *116*, 264–273. https://doi.org/10.1016/j.geomorph.2009.11.012

Maxwell, A. E., Warner, T. A., Vanderbilt, B. C., & Ramezan, C. A. (2017). Land cover classification and feature extraction from National Agriculture Imagery Program (NAIP) Orthoimagery: A review. *Photogrammetric Engineering and Remote Sensing*, *83*(11), 737–747. https://doi.org/10.14358/PERS.83.10.737

McLaughlin, B. C., Ackerly, D. D., Klos, P. Z., Natali, J., Dawson, T. E., & Thompson,

S. E. (2017). Hydrologic refugia, plants, and climate change. *Global Change Biology*, *23*(8), 2941–2961. https://doi.org/10.1111/gcb.13629

Näsi, R., Honkavaara, E., Lyytikäinen-Saarenmaa, P., Blomqvist, M., Litkey, P., Hakala, T., Viljanen, N., Kantola, T., Tanhuanpää, T., & Holopainen, M. (2015). Using UAV-Based Photogrammetry and Hyperspectral Imaging for Mapping Bark Beetle Damage at Tree-Level. *Remote Sensing*, *7*, 15467–15493. https://doi.org/10.3390/rs71115467

North, M. P., Kane, J. T., Kane, V. R., Asner, G. P., Berigan, W., Churchill, D. J., Conway, S., Gutiérrez, R. J., Jeronimo, S., Keane, J., Koltunov, A., Mark, T., Moskal, M., Munton, T., Peery, Z., Ramirez, C., Sollmann, R., White, A., & Whitmore, S. (2017). Cover of tall trees best predicts California spotted owl habitat. *Forest Ecology and Management*, *405*(July), 166–178. https://doi.org/10.1016/j.foreco.2017.09.019

Noss, R. (2000). The Redwood Forest: History, Ecology, and Conservation of the Coast Redwoods. *Bibliovault OAI Repository, the University of Chicago Press*.

Olson, D. F., Douglass, R. F., & Walters, G. A. (1990). Sequoia sempervirens. *In Silvics of North America, Volume 1, Conifers. USDA Forest Service Handbook*, 654.

Pau, G., Fuchs, F., Sklyar, O., Boutros, M., & Huber, W. (2010). EBImage—an R package for image processing with applications to cellular phenotypes. *Bioinformatics*, *26*(7), 979–981. https://doi.org/10.1093/bioinformatics/btq046

Pittermann, J., Stuart, S. A., Dawson, T. E., & Moreau, A. (2012). Cenozoic climate change shaped the evolutionary ecophysiology of the Cupressaceae conifers. *Proceedings of the National Academy of Sciences*, *109*(24), 9647–9652.

https://doi.org/10.1073/pnas.1114378109

R Core Team. (2018). *R: A Language and Environment for Statistical Computing*. https://www.r-project.org/

Riley, S. J., DeGloria, S. D., & Elliot, R. (1999). A Terrain Ruggedness that Quantifies Topographic Heterogeneity. *Intermountain Journal of Science*, *5*(1–4), 23–27.

Roden, J. S., Johnstone, J. A., & Dawson, T. E. (2009). Intra-annual variation in the stable oxygen and carbon isotope ratios of cellulose in tree rings of coast redwood (Sequoia sempervirens). *Holocene*, *19*(2), 189–197. https://doi.org/10.1177/0959683608098959

Roussel, J.-R., & Auty, D. (2020). *lidR: Airborne LiDAR Data Manipulation and Visualization for Forestry Applications*. https://cran.r-project.org/package=lidR

Russell, W. H., McBride, J. R., & Carnell, K. (2000). Edge effects and the effective size of old-growth coast redwood preserves. *Proceedings Rocky Mountain Research Station, USDA Forest Service*, *3*, 128–136. https://www.fs.usda.gov/treesearch/pubs/21978

Sawyer, J. O., Sillett, S. C., Popenoe, J. H., LaBanca, A., Sholars, T., Largent, D. L., Euphrat, F., Noss, R. F., & Van Pelt, R. (2000). Characteristics of redwood forests. In *The Redwood Forest: History, Ecology, and Conservation of the Coast Redwoods.* (pp. 39–79). Island Press.

Sillett, S. C., & Van Pelt, R. (2000). Tree Whose Crown is a Forest Canopy. *Northwest Science*, *74*(1), 34–43.

Sillett, S. C., & Van Pelt, R. (2007). Trunk Reiteration Promotes Epiphytes and Water Storage in an Old-Growth Redwood Forest. *Ecological Monographs*, *77*(3), 335–

359.

Sillett, S. C., Van Pelt, R., Carroll, A. L., Campbell-Spickler, J., Coonen, E. J., & Iberle, B. G. (2019). Allometric equations for Sequoia sempervirens in forests of different ages. *Forest Ecology and Management*, *433*, 349–363. https://doi.org/10.1016/j.foreco.2018.11.016

Sillett, S. C., Van Pelt, R., Carroll, A. L., Kramer, R. D., Ambrose, A. R., & Trask, D. (2015). How do tree structure and old age affect growth potential of california redwoods? *Ecological Monographs*, *85*(2), 181–212. https://doi.org/10.1890/14-1016.1

Sillett, S. C., Van Pelt, R., Koch, G. W., Ambrose, A. R., Carroll, A. L., Antoine, M. E., & Mifsud, B. M. (2010). Increasing wood production through old age in tall trees. *Forest Ecology and Management*, *259*(5), 976–994. https://doi.org/https://doi.org/10.1016/j.foreco.2009.12.003

Stone, E. C., & Vasey, R. B. (1968). Preservation Of Coast Redwood on Alluvial Flats. *Science*, *159*(3811), 157–161.

Tucker, C. J. (1979). Red and photographic infrared linear combinations for monitoring vegetation. *Remote Sensing of Environment*, *7*, 127–150.

Tyree, M. T., & Sperry, J. S. (1988). Do Woody Plants Operate Near the Point of Catastrophic Xylem Dysfunction Caused by Dynamic Water Stress? *Plant Physiology*, *88*(3), 574 LP – 580. https://doi.org/10.1104/pp.88.3.574

USGS. (2020). *USGS Lidar Point Cloud CA NoCAL Wildfires B4 2018*. U.S. Geological Survey.

Van Pelt, R., Sillett, S. C., Kruse, W. A., Freund, J. A., & Kramer, R. D. (2016).

Emergent crowns and light-use complementarity lead to global maximum biomass and leaf area in Sequoia sempervirens forests. *Forest Ecology and Management*, *375*, 279–308. https://doi.org/10.1016/j.foreco.2016.05.018

https://doi.org/10.1109/34.87344

Voelker, S. L., Roden, J. S., & Dawson, T. E. (2018). Millennial-scale tree-ring isotope chronologies from coast redwoods provide insights on controls over California hydroclimate variability. *Oecologia*, *187*(4), 897–909. https://doi.org/10.1007/s00442-018-4193-4

Wulder, M. A., Dymond, C. C., White, J. C., Leckie, D. G., & Carroll, A. L. (2006). Surveying mountain pine beetle damage of forests: A review of remote sensing opportunities. *Forest Ecology and Management*, *221*(1–3), 27–41. https://doi.org/10.1016/j.foreco.2005.09.021

Tables and Figures

Table 3-1: Confusion matrix results for the random forest classification of the 2016 NAIP imagery

NAIP 2016 Random Forest Classification

	Dieback	**Healthy**	**Shadow**	**Users Accuracy:**
Dieback	200	0	0	100.0%
Healthy	1	224	0	99.6%
Shadow	0	0	200	100.0%
Producers Accuracy:	99.5%	100.0%	100.0%	
Overall Accuracy:	99.84%			
Cohen's Kappa:	0.9976			

Table 3-2: Confusion matrix results for the random forest classification of the 2018 NAIP imagery.

NAIP 2018 Random Forest Classification

	Dieback	**Healthy**	**Shadow**	**Users Accuracy:**
Dieback	200	0	0	100.0%
Healthy	0	225	0	100.0%
Shadow	0	0	200	100.0%
Producers Accuracy:	100%	100%	100%	
Overall Accuracy:	100%			
Cohen's Kappa:	1			

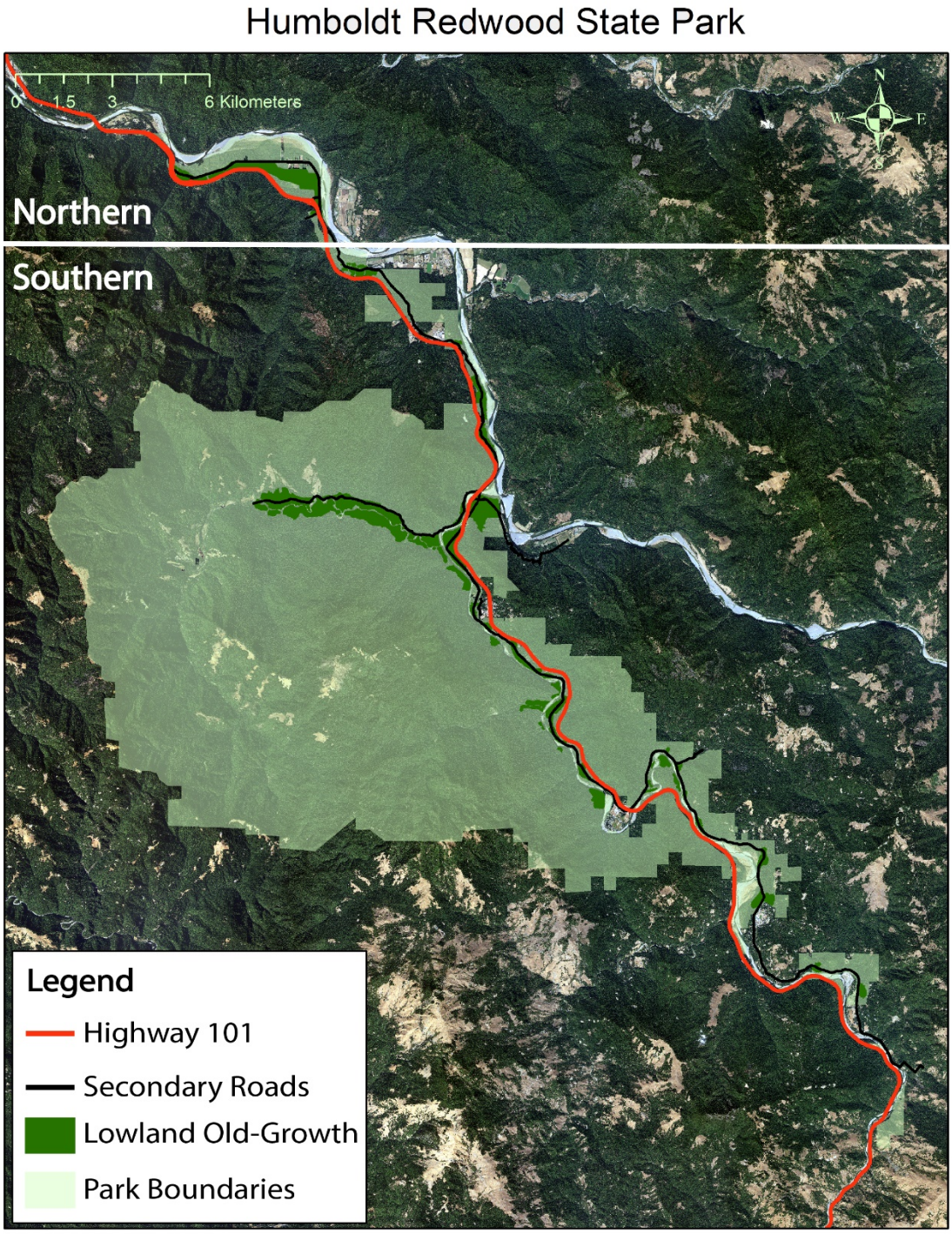

Figure 3-1: Map of Humboldt Redwood State Park (light green) and the public roadways, including Highway 101 (red line) and other secondary roads including the Avenue of the Giants (black lines) that bisect the park. We restricted our study area to the lowland areas of the park that contain old-growth redwood forest (dark green). Analyses were conducted separately on the northern (above the white line) and southern regions (below the white line) based on the prevalence of dieback (Figure B-2).

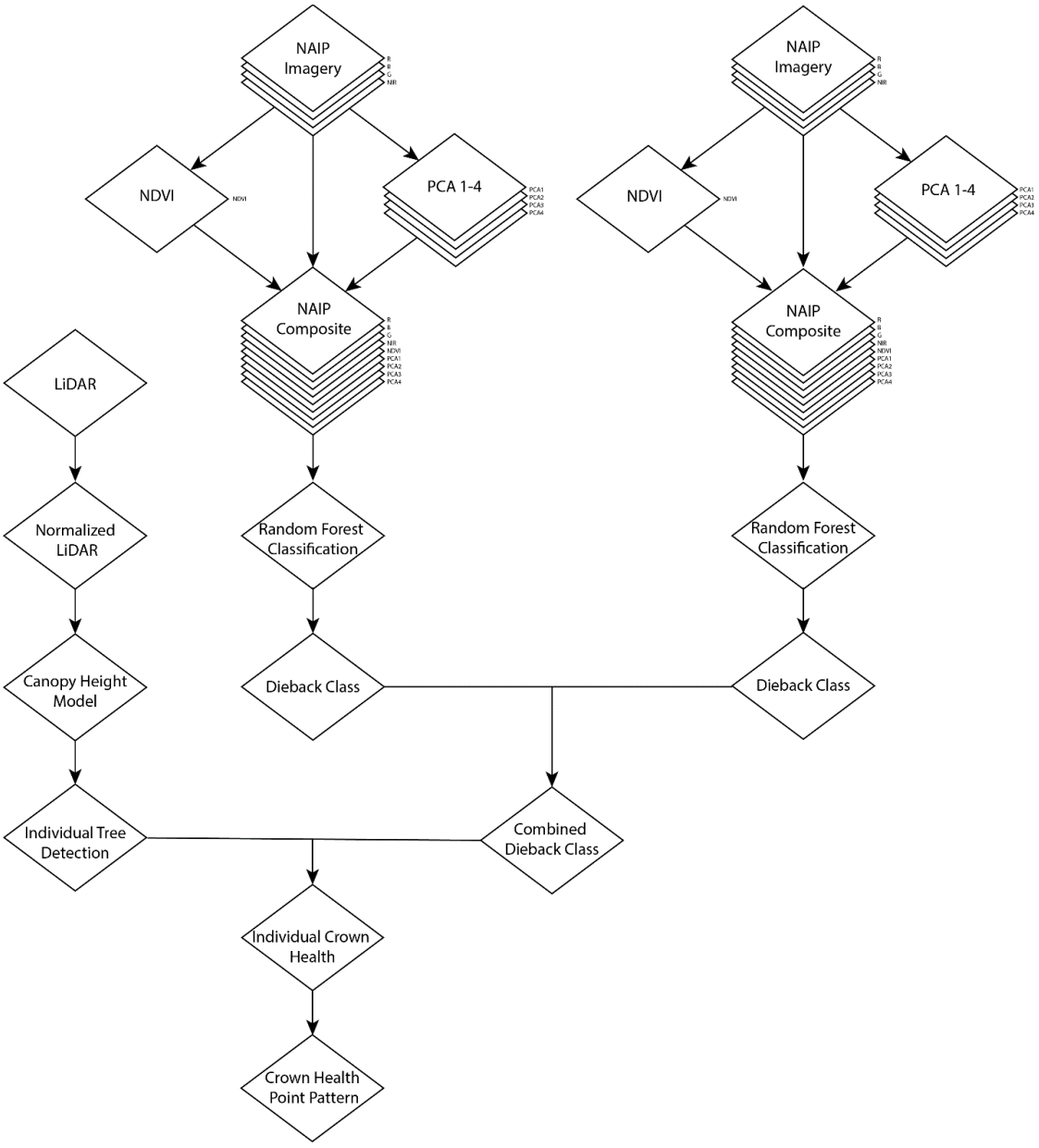

Figure 3-2: Workflow chart documenting the steps taken to create a spatial point pattern of crown health using NAIP imagery and discrete-return aerial LiDAR.

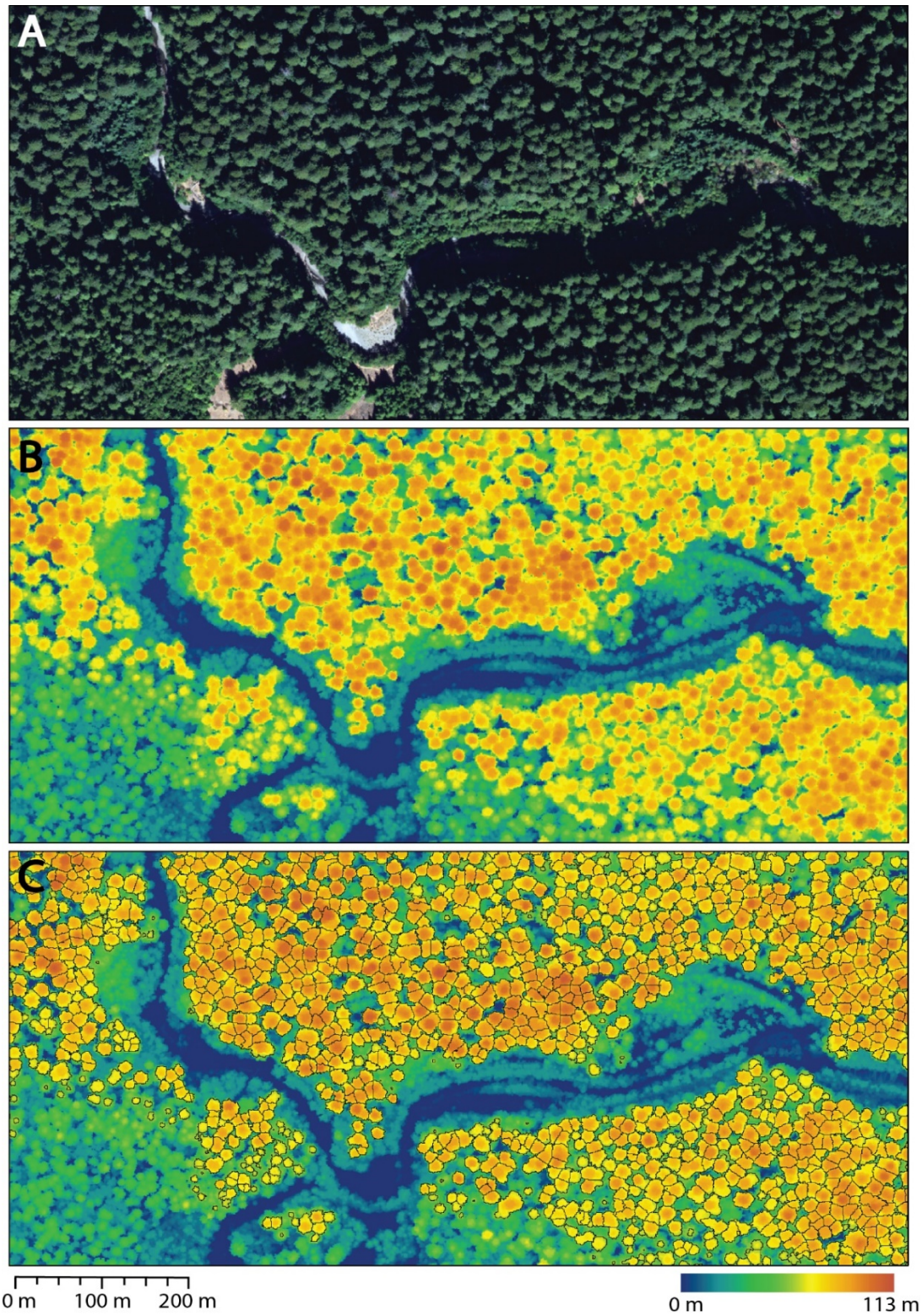

Figure 3-3: Aerial views of (A) 2018 NAIP imagery in natural color composite, (B) LiDAR-derived Canopy Height Model, and (C) individual tree segmentation of canopy dominant trees.

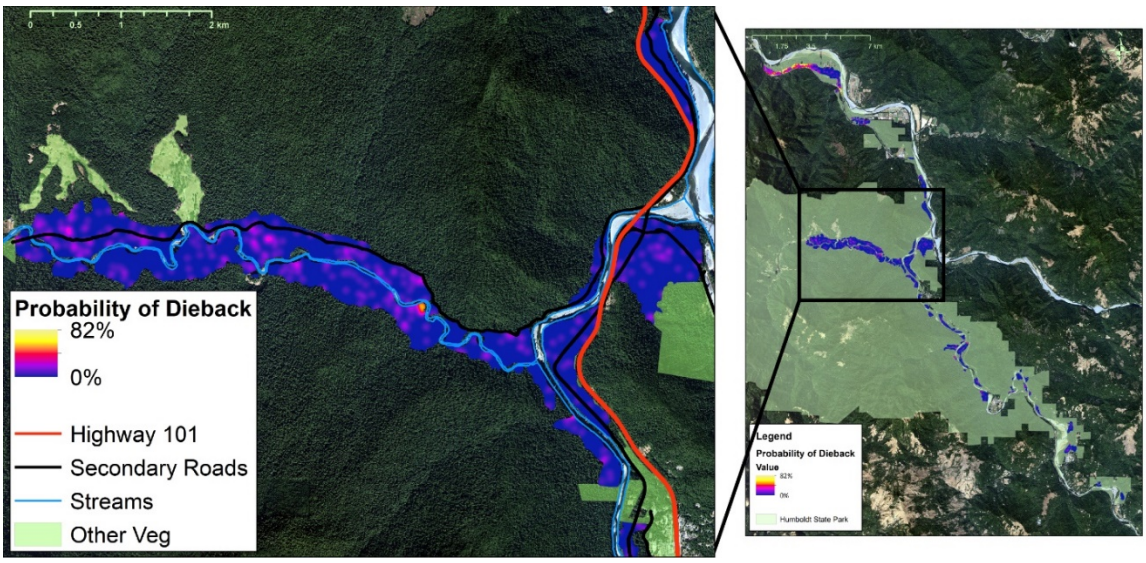

Figure 3-4: Probability of crown dieback in the southern portion of the park containing Bull Creek and the Rockefeller Forest area.

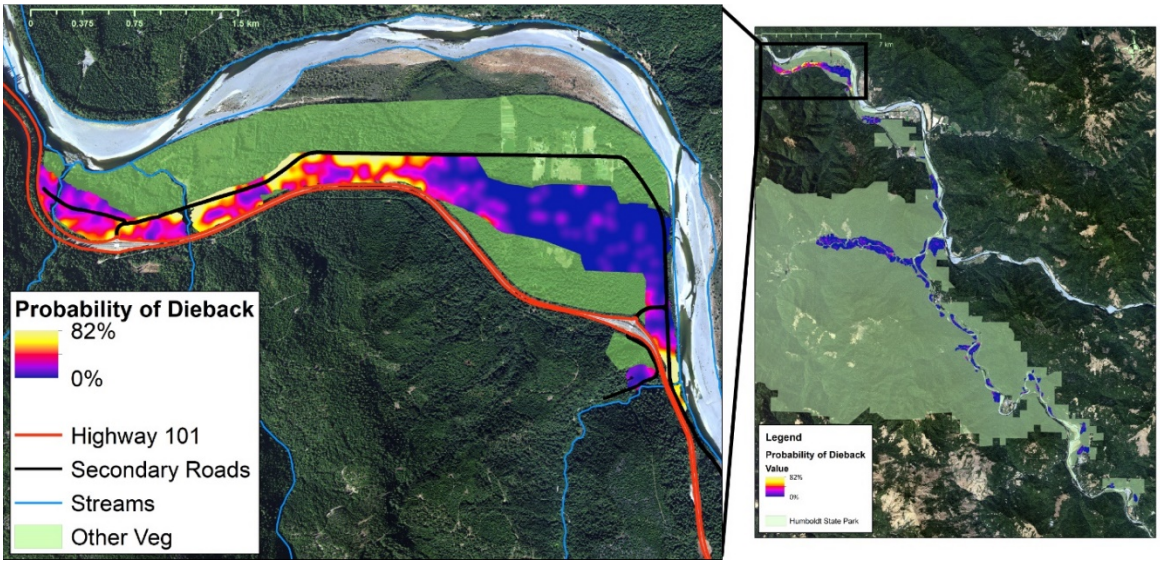

Figure 3-5: Probability of crown dieback in the northern portion of the park.

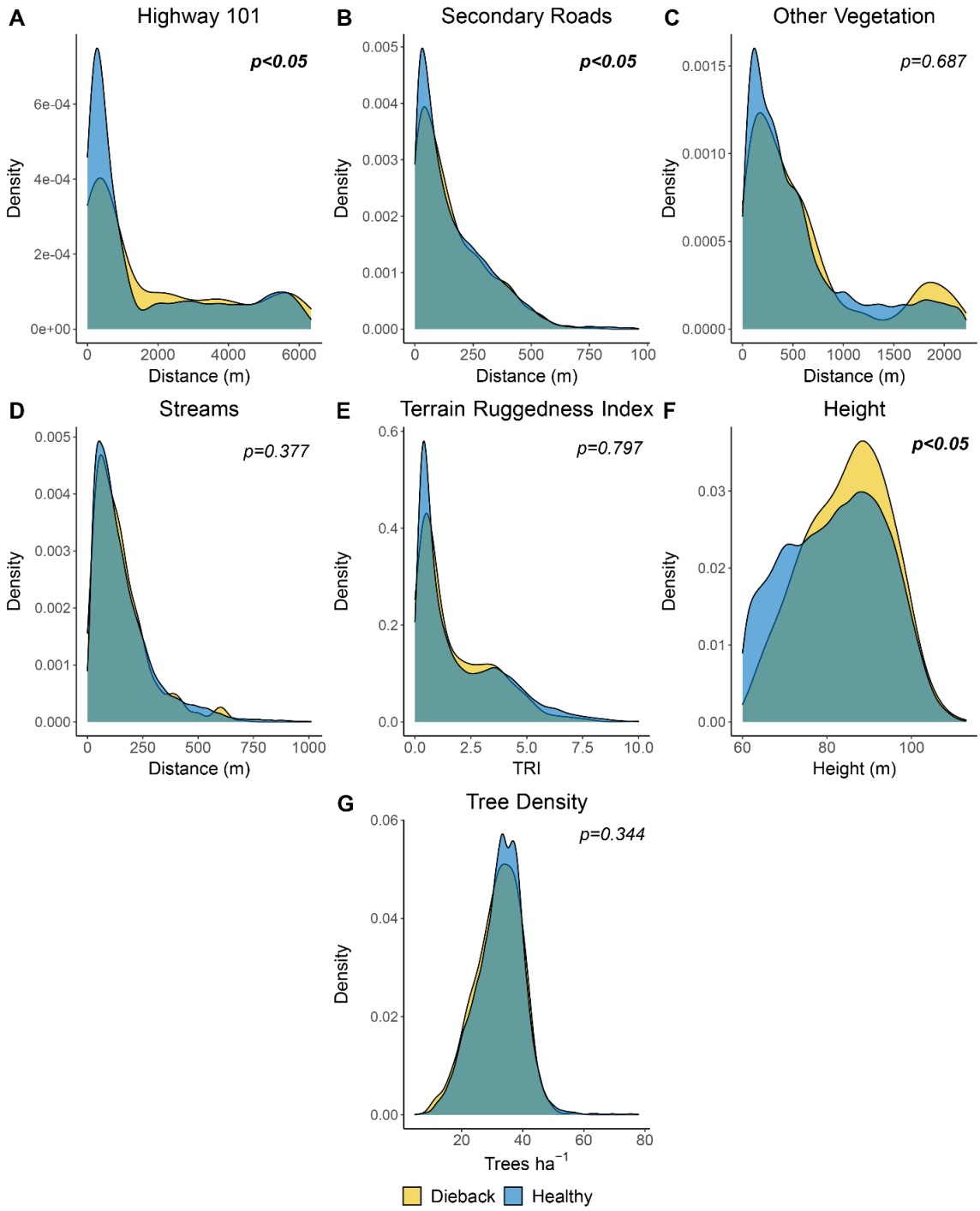

Figure 3-6: Variable distribution comparisons for trees from the southern portion of the park. Panels show the density of healthy (blue) or dieback (yellow) trees near (A-D) different edge features, (E) the ruggedness of the surrounding topography, (F) individual tree height, and (G) overall tree density. Differences between each variable distribution is shown below each comparison and were tested using a two-sample Kolmogorov-Smirnov test ($p<0.05$).

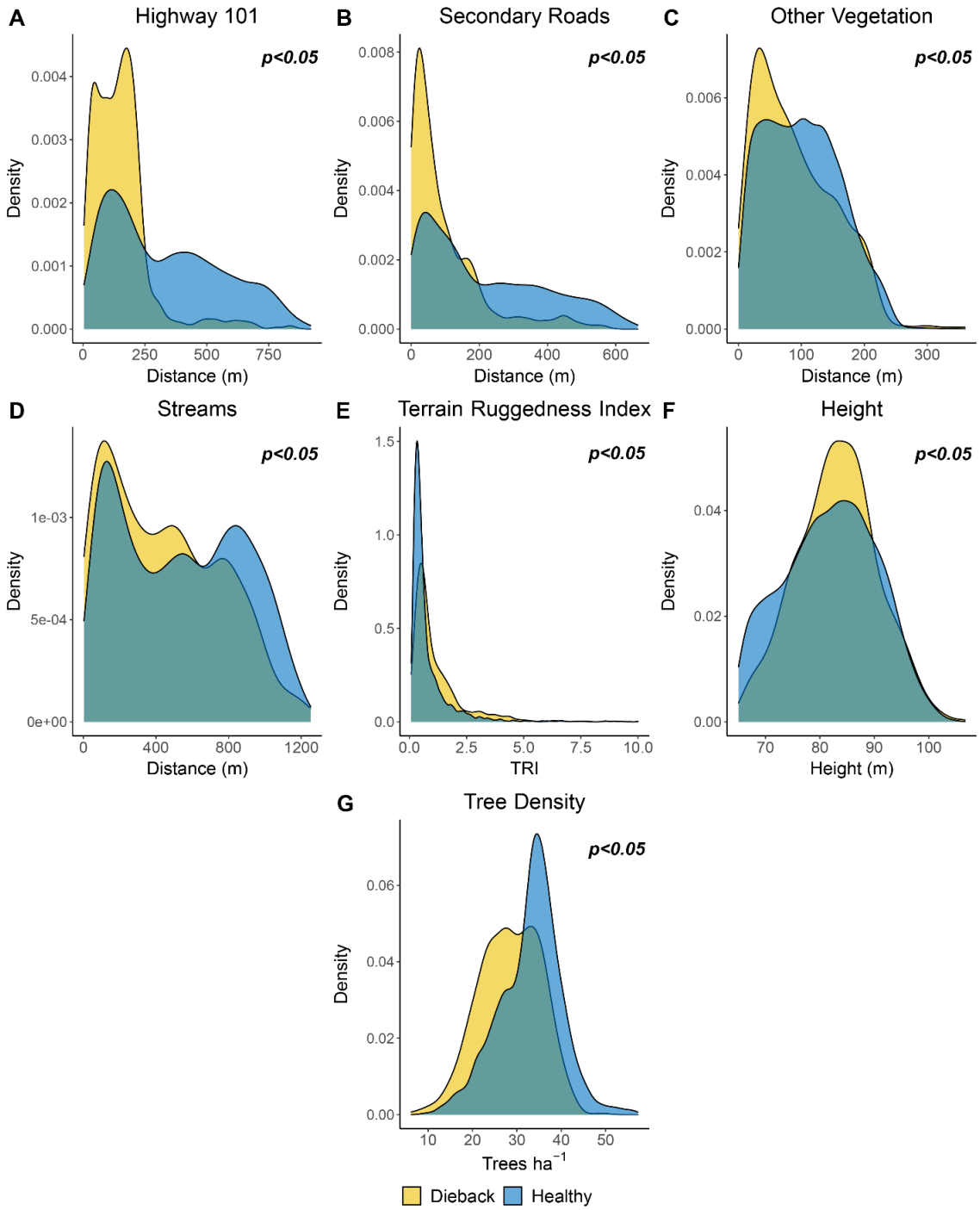

Figure 3-7: Variable distribution comparisons for trees from the northern portion of the park. Panels show the density of healthy (blue) or dieback (yellow) trees near (A-D) different edge features, (E) the ruggedness of the surrounding topography, (F) individual tree height, and (G) overall tree density. Differences between each variable distribution is shown below each comparison and were tested using a two-sample Kolmogorov-Smirnov test ($p<0.05$).

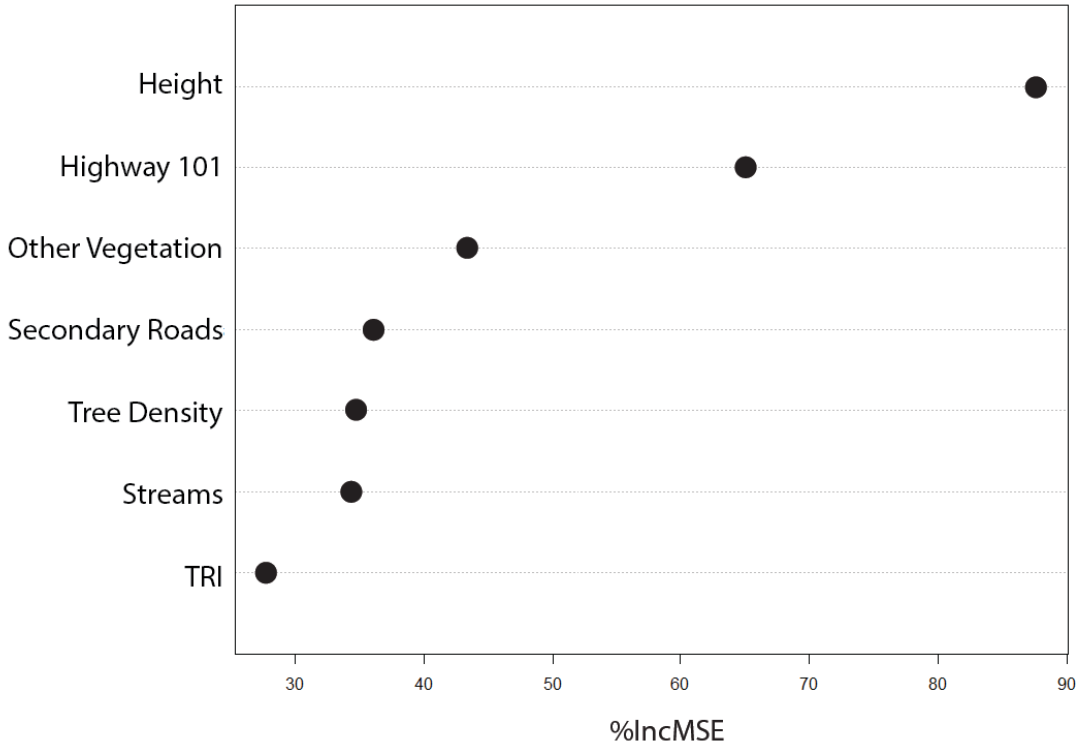

Figure 3-8: The relative variable importance for the RF analysis of the northern portion of the park. Each variable is ranked based on the measured increase of mean standard error (%IncMSE) when excluded from the RF model. Terrain ruggedness index is represented by TRI.

CHAPTER 4

SUMMARY AND CONCLUSIONS

For the past two centuries, the coast redwood ecosystem has been heavily fragmented, making remaining redwoods more susceptible to elevated wind and light intensities which have been linked with increased rates of windrow and crown dieback (Laurance et al., 2007; 2009; Laurance & Curran, 2008; Russell et al., 2000). While conservation efforts and establishment of large preservation efforts for the remaining old growth redwood forest, it remains unknown how edge effects permeate remaining redwood stands and how these effects impact stand health and composition. In this thesis, I combined methods from dendrochronology with remote sensing to document temporal and spatial changes in the health and productivity of old-growth coast redwoods as they relate to anthropogenic edges and stand demographics.

In the second chapter, we were interested in using tree-ring data to identify the changes in growth and ecophysiology in old redwoods that could be uniquely attributed to previous road expansions. Increment cores were extracted from plots that had different proximities to edge disturbances, and we contrasted their growth and stable isotopes to identify potential disturbance signals recorded in the tree-rings. Consistent with previous studies that have attempted to use redwoods for dendrochronological research, crossdating of increment cores proved to be difficult due to anomalous growth patterns that frequent redwood cores (Brown & Swetnam, 1994; Carroll et al., 2018). We also found that there were similarities in growth suppression in plots regardless of proximity to forest edge or similar geographic distance within the park. The commonality of these suppressions in different areas of our study area suggest that many of the more ephemeral

suppression patterns throughout our time series were largely driven climatic variation. However, asynchronous patterns suggested that previous road construction activities disproportionality impacted the growth of trees that were within 30 m of the highway and growth suppressions were particularly severe in trees that exhibited crown dieback. Moreover, our analyses of stable carbon isotopes suggested that previous road installations also led to elevated levels drought stress for several decades for bordering trees.

In the third chapter, we used remote sensing data to map crown health at the individual tree-level to analyze the spatial patterns and potential drivers of crown dieback. We found that we were able to accurately identify crown health of individual redwood using publicly available aerial imagery and Light Detection and Ranging (LiDAR) data. We found that tree height was the most important variable for describing the patterns of crown dieback. The prevalence of crown dieback in taller trees is likely attributable to the increased sunlight and wind exposure of these trees in addition to the constraints that height places on maintain a water column (Domec et al., 2010; Koch et al., 2004). These findings are consistent with other studies that have found that taller trees have been more susceptible to drought-related mortality and edge effects (Bennett et al., 2015; Laurance & Curran, 2008). We also found that crown dieback varied spatially across our study area. For most of our study area, crown dieback was relatively low, however in some areas crown dieback was heavily concentrated. In these areas, crown dieback aggregated in areas near forest edges and in areas with low tree density. It is possible that the drivers of crown deterioration and lower tree density are the same because the increased risk of windthrow (Laurance & Curran, 2008), the leading cause of

mortality in redwoods (Van Pelt et al., 2016), however further research is needed to verify this hypothesis.

While the redwood has an unusually large number of traits have previously made them robust and resilient to many different types of natural disturbances (Lorimer et al., 2009), they also have many traits that make them potentially intolerant of the pressures associated with forest edges and a changing climate (Burgess & Dawson, 2004; Dawson et al., 2007; Fernández et al., 2015; Johnstone & Dawson, 2010; Russell et al., 2000). By conducting this study, we hoped to elucidate the responses that coast redwoods have had to anthropogenic disturbances and provide valuable insight for the prioritize conservation efforts in areas that may have been particularly impacted by previous activities. We also hope that methodologies used in this study may prove to be useful for land and park managers seeking to conduct large-scale health assessments of redwoods in other parks and preserves in the near future.

References

Bennett, A. C., Mcdowell, N. G., Allen, C. D., & Anderson-teixeira, K. J. (2015). *Larger trees suffer most during drought in forests worldwide*. *September*, 1–5. https://doi.org/10.1038/NPLANTS.2015.139

Brown, P., & Swetnam, T. (1994). A cross-dated fire history from coast redwood near Redwood National Park, California. *Canadian Journal of Forest Research*, *24*, 21–31. https://doi.org/10.1139/x94-004

Burgess, S., & Dawson, T. E. (2004). The contribution of fog to the water relations of Sequoia sempervirens (D. Don): Foliar uptake and prevention of dehydration. *Plant, Cell and Environment*, *27*, 1023–1034. https://doi.org/10.1111/j.1365-

3040.2004.01207.x

Carroll, A. L., Sillett, S. C., Palladini, M., & Campbell-Spickler, J. (2018). Dendrochronological analysis of Sequoia sempervirens in an interior old-growth forest. *Dendrochronologia*, *52*, 29–39. https://doi.org/10.1016/j.dendro.2018.09.006

Dawson, T. E., Burgess, S. S. O., Tu, K. P., Oliveira, R. S., Santiago, L. S., Fisher, J. B., Simonin, K. A., & Ambrose, A. R. (2007). Nighttime transpiration in woody plants from contrasting ecosystems. *Tree Physiology*, *27*(4), 561–575. https://doi.org/10.1093/treephys/27.4.561

Domec, J. C., Schäfer, K., Oren, R., Kim, H. S., & McCarthy, H. R. (2010). Variable conductivity and embolism in roots and branches of four contrasting tree species and their impacts on whole-plant hydraulic performance under future atmospheric CO2 concentration. *Tree Physiology*, *30*(8), 1001–1015. https://doi.org/10.1093/treephys/tpq054

Fernández, M., Hamilton, H. H., & Kueppers, L. M. (2015). Back to the future: using historical climate variation to project near-term shifts in habitat suitable for coast redwood. *Global Change Biology*, *21*(11), 4141–4152. https://doi.org/10.1111/gcb.13027

Johnstone, J. A., & Dawson, T. E. (2010). Climatic context and ecological implications of summer fog decline in the coast redwood region. *Proceedings of the National Academy of Sciences of the United States of America*, *107*(10), 4533–4538. https://doi.org/10.1073/pnas.0915062107

Koch, G. W., Stillet, S. C., Jennings, G. M., & Davis, S. D. (2004). The limits to tree

height. *Nature*, *428*(6985), 851–854. https://doi.org/10.1038/nature02417

Laurance, W. F., & Curran, T. J. (2008). Impacts of wind disturbance on fragmented tropical forests: A review and synthesis. *Austral Ecology*, *33*, 399–408. https://doi.org/10.1111/j.1442-9993.2008.01895.x

Laurance, W. F., Goosem, M., & Laurance, S. G. W. (2009). Impacts of roads and linear clearings on tropical forests. *Trends in Ecology and Evolution*, *24*(12), 659–669. https://doi.org/10.1016/j.tree.2009.06.009

Laurance, W. F., Nascimento, H. E. M., Laurance, S. G., Andrade, A., Ewers, R. M., Harms, K. E., Luizão, R. C. C., & Ribeiro, J. E. (2007). Habitat fragmentation, variable edge effects, and the landscape-divergence hypothesis. *PLoS ONE*, *2*(10). https://doi.org/10.1371/journal.pone.0001017

Lorimer, C. G., Porter, D. J., Madej, M. A., Stuart, J. D., Veirs, S. D., Norman, S. P., O'Hara, K. L., & Libby, W. J. (2009). Presettlement and modern disturbance regimes in coast redwood forests: Implications for the conservation of old-growth stands. *Forest Ecology and Management*, *258*(7), 1038–1054. https://doi.org/10.1016/j.foreco.2009.07.008

Russell, W. H., McBride, J. R., & Carnell, K. (2000). Edge effects and the effective size of old-growth coast redwood preserves. *Proceedings Rocky Mountain Research Station, USDA Forest Service*, *3*, 128–136. https://www.fs.usda.gov/treesearch/pubs/21978

Van Pelt, R., Sillett, S. C., Kruse, W. A., Freund, J. A., & Kramer, R. D. (2016). Emergent crowns and light-use complementarity lead to global maximum biomass and leaf area in Sequoia sempervirens forests. *Forest Ecology and*

Management, *375*, 279–308. https://doi.org/10.1016/j.foreco.2016.05.018

APPENDICIES

APPENDIX A

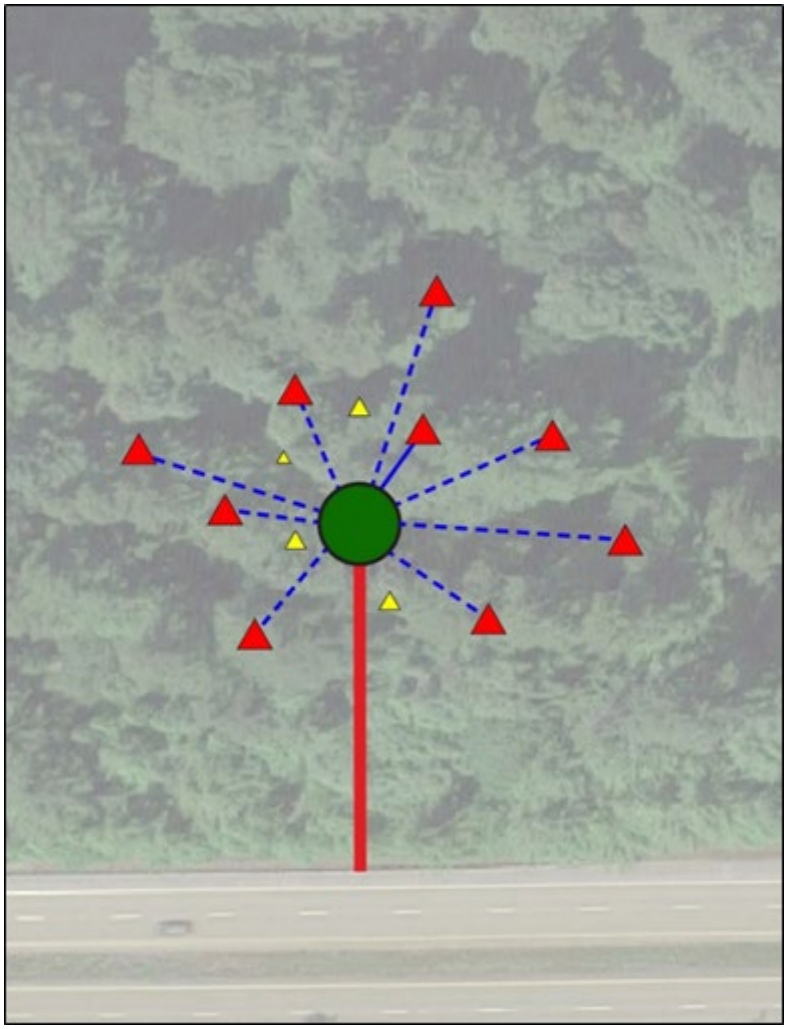

Figure A-1: Sampling design and tree selection at each plot. Both the angle and distance to edge (red line) were selected at random. The green dot represents the central tree at each plot. The surrounding nine red triangles represent the closest trees that were also selected. Yellow triangles represent trees that were excluded from sampling due to sub-dominant canopy positioning.

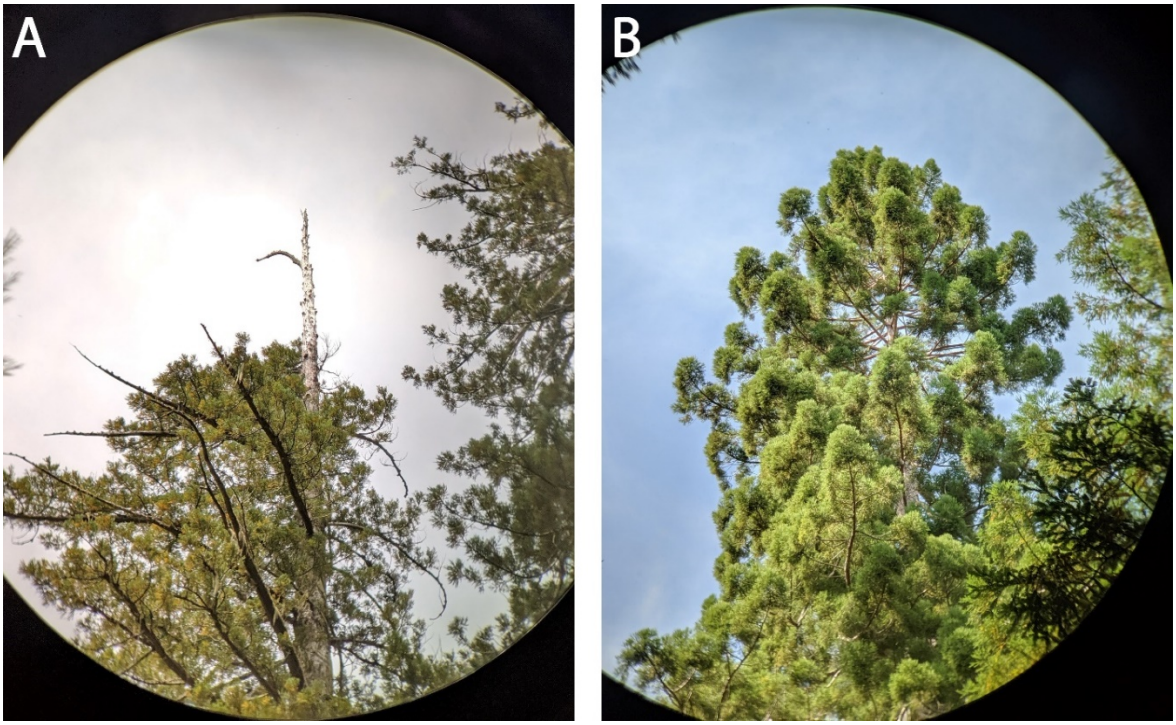

Figure A-2: Examples of trees with (A) crown dieback and (B) healthy crowns.

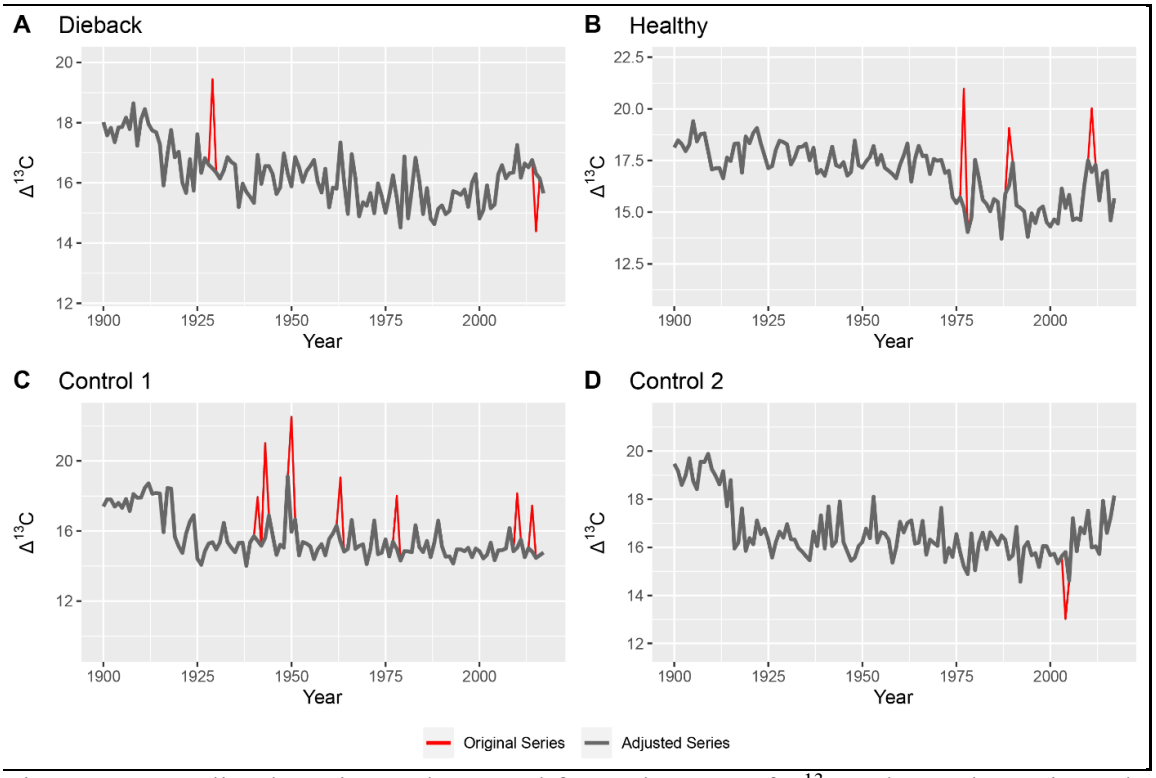

Figure A-3: Outlier detection and removal for each group of $\Delta^{13}C$ values. Shown in each plot are original $\Delta^{13}C$ values (red lines) and adjusted $\Delta^{13}C$ values after outlier removal (grey lines). (A) Dieback trees adjacent to the road. (B) Healthy trees adjacent to the road. (C) Control 1 trees located near Bull Creek in the Rockefeller forest. (D) Control 2 trees located near Pepperwood, CA.

APPENDIX B

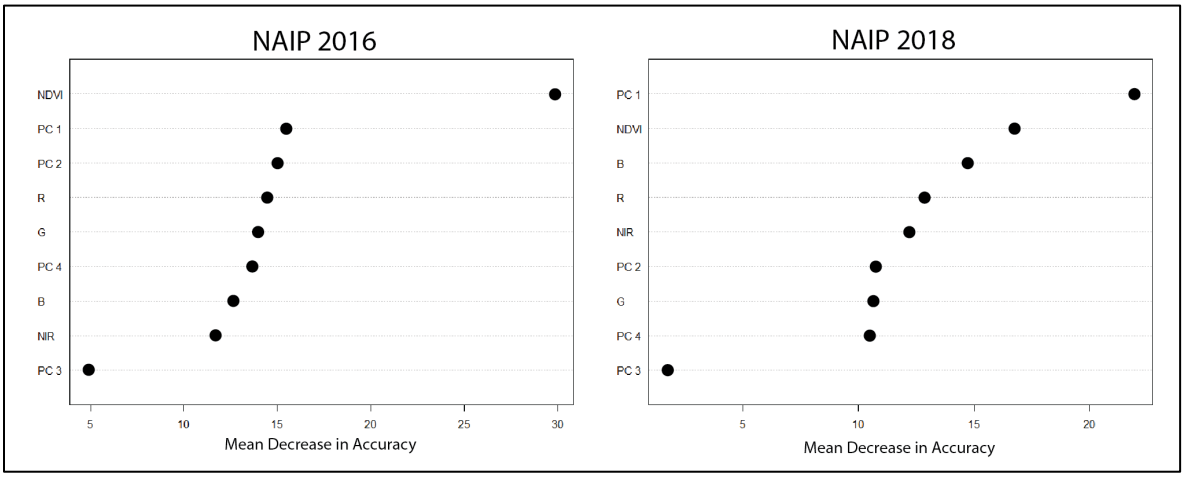

Figure B-1: Relative variable importance for each random forest classification. For both classifications, NDVI and PC 1 were the top two most important variables for discerning our classes (crown dieback, healthy crown, and shadow).

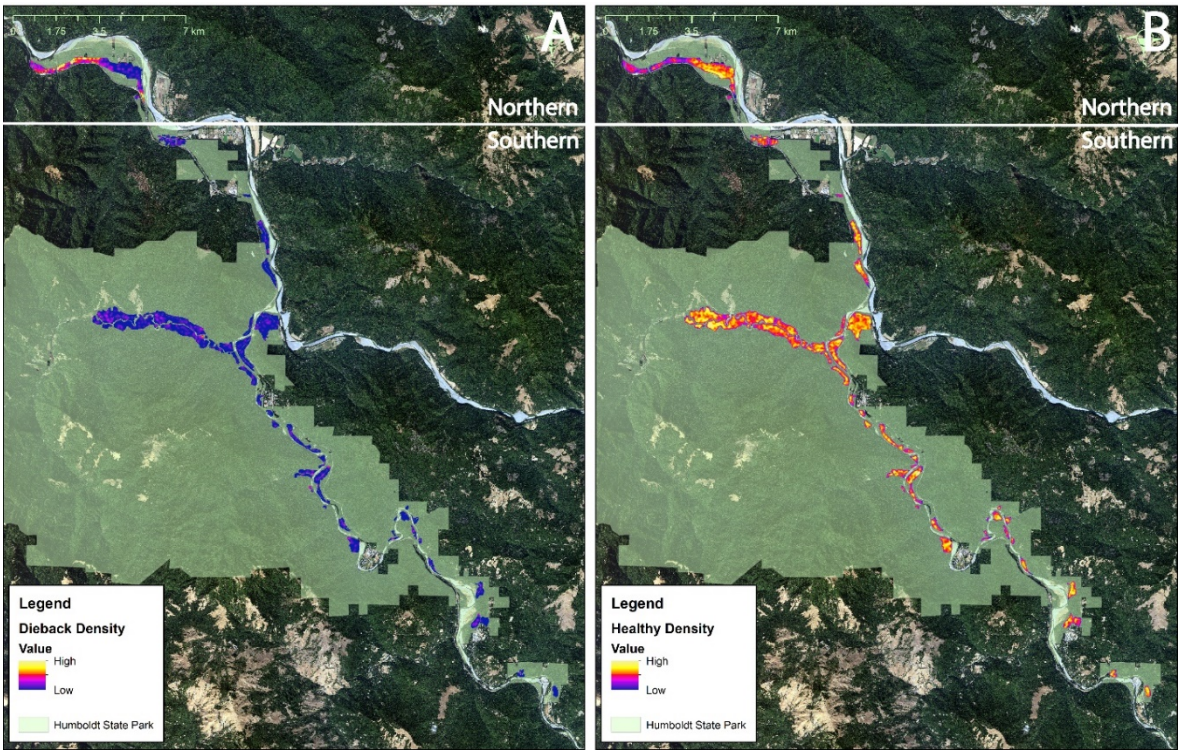

Figure B-2: Kernel density estimation of trees split based on crown health. (A) The density of trees with crown dieback is heavily aggregated in the northern portion of the park, whereas, (B) the density of health trees is relatively consistent throughout the study area.

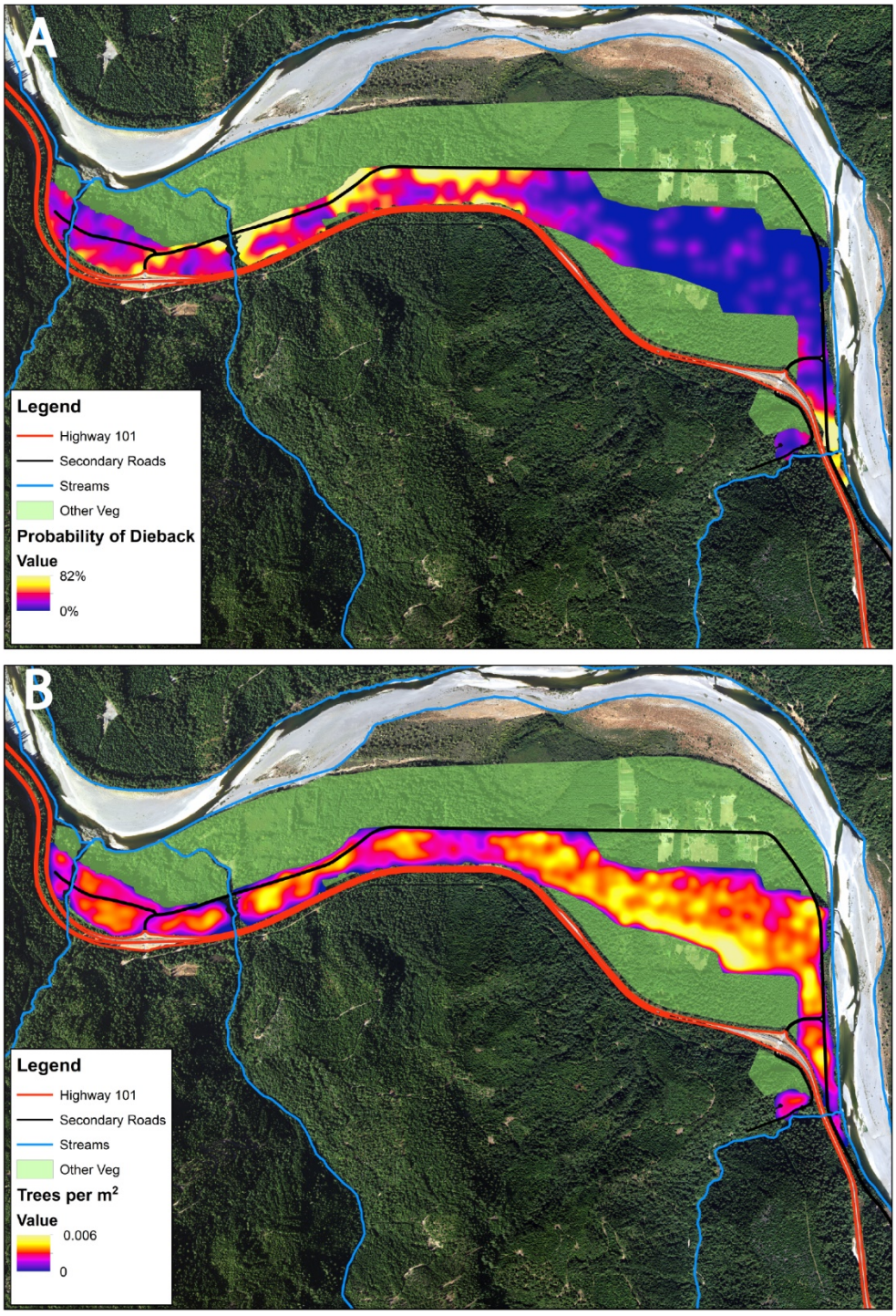

Figure B-3: (A) Probability of crown dieback in the northern portion of the park. (B) Overall tree kernel density.